

Spatial $\Sigma\Delta$ Modulation in a Massive MIMO Cellular System

A signal processing investigation of spatial $\Sigma\Delta$ modulation

Master's thesis in Embedded Electronic System Design

DAVOR BARAC
EMIL LINDQVIST

MASTER'S THESIS 2016

Design and Evaluation of a $\Sigma\Delta$ Modulator ADC Utilizing The Spatial Dimension

An investigation of how the spatial dimension can
be used in a $\Sigma\Delta$ modulator to reduce the bandwidth
requirement in a receiver with hundreds of antennas

DAVOR BARAC
EMIL LINDQVIST

Department of Computer Science and Engineering
Division of Computer Engineering
CHALMERS UNIVERSITY OF TECHNOLOGY
UNIVERSITY OF GOTHENBURG
Gothenburg, Sweden 2016

Design and Evaluation of a $\Sigma\Delta$ Modulator ADC Utilizing The Spatial Dimension
An investigation of how the spatial dimension can be used in a $\Sigma\Delta$ modulator to reduce
the bandwidth requirement in a receiver with hundreds of antennas
DAVOR BARAC
EMIL LINDQVIST

© DAVOR BARAC, 2016.
© EMIL LINDQVIST, 2016.

Supervisor: Lars Svensson, Department of Computer Science and Engineering
Ulf Gustavsson, Ericsson
Examiner: Per Larsson-Edefors, Department of Computer Science and Engineering

Master's Thesis 2016
Department of Computer Science and Engineering
Division of Computer Engineering
Chalmers University of Technology
University of Gothenburg
SE-412 96 Gothenburg
Telephone +46 31 772 1000

Cover: Spatio-temporal $\Sigma\Delta$ modulator which can shape the quantization noise in space

Typeset in L^AT_EX
Gothenburg, Sweden 2016

Design and Evaluation of a $\Sigma\Delta$ Modulator ADC Utilizing The Spatial Dimension
An investigation of how the spatial dimension can be used in a $\Sigma\Delta$ modulator to reduce the bandwidth requirement in a receiver with hundreds of antennas

DAVOR BARAC

EMIL LINDQVIST

Department of Computer Science and Engineering

Chalmers University of Technology

University of Gothenburg

Abstract

In cellular networks, frequency channels are used to separate the users. However frequency spectrum is an ever-decreasing resource as wireless units and applications increase. Thus, other means to separate the users are of interest. By using hundreds of antennas and beamforming in the system, the users can be efficiently multiplexed in the spatial domain, while using the same time-frequency resource. The large amount of antennas however requires extensive data processing and transport which is difficult and expensive to handle. Thus, an investigation of how to reduce the data bandwidth required in such a system is of interest. This master thesis project evaluates the use of the spatial dimension in a $\Sigma\Delta$ modulator as part of the analog-to-digital conversion. It is put into the context of beamforming and evaluated.

A simulator developed in MATLAB is utilized to show the properties and qualities of different modulator structures in a beamforming application. In particular, performance at low converter speeds is evaluated.

The results show that by using the spatial dimension in a $\Sigma\Delta$ modulator it is possible to reduce the bandwidth requirement, through reduction of sampling rate while still retaining the signal quality. However, this is applicable only in one direction at a time, and there are multiple implementation issues regarding the proposed design.

The findings suggest that with the spatial dimension in a $\Sigma\Delta$ modulator there are possibilities to reduce the bandwidth requirement in antenna array systems but that there are considerable challenges to overcome.

Keywords: sigma-delta modulation, spatial, multi-antenna array, signal processing, beamforming, miso.

Acknowledgements

We would like to thank our supervisors Lars Svensson at Chalmers and Ulf Gustavsson at Ericsson for an interesting, challenging and fun master's thesis project. Ulf Gustavsson has provided very valuable insight into telecom systems and has been a bit of a walking reference book. Lars Svensson has guided our work and kept things down-to-earth, but above all he has inspired us in ways far beyond the scope of this master's thesis. It is truly awesome to have a teacher and supervisor who loves what he does and actually cares; a true role model in a lot of ways.

Finally, we want to thank our families for being supportive and motivating us through all years of studies.

Davor & Emil, Gothenburg, June 2016

Acronyms

- **ADC** - Analog-to-Digital Converter
- **IC** - Integrated Circuit
- **SIMO** - Single Input Multiple Output
- **MISO** - Multiple Input Single Output
- **MIMO** - Multiple Input Multiple Output
- **MRC** - Maximum Ratio Combining
- **RMS** - Root Mean Square
- **STF** - Signal Transfer Function
- **NTF** - Noise Transfer Function
- **SNR** - Signal-to-Noise Ratio
- **OSR** - Oversampling Ratio
- **NMSE** - Normalized Mean Square Error

Contents

1	Introduction	1
2	Theory	3
2.1	Wireless communication	3
2.2	Beamforming	4
2.2.1	Principle	4
2.2.2	Spatial selectivity	7
2.3	The temporal $\Sigma\Delta$ modulator	9
2.3.1	Introduction	9
2.3.2	System models	9
2.3.3	Mathematical expressions	11
2.3.4	Example	12
2.4	The spatial $\Sigma\Delta$ modulator	14
2.4.1	Introduction	14
2.4.2	System models	14
2.4.3	Algebraic analysis	14
2.4.4	Second-order spatial $\Sigma\Delta$ modulator	16
2.5	The spatio-temporal $\Sigma\Delta$ modulator	17
2.6	$\Sigma\Delta$ modulation in a beamforming application	18
2.6.1	System model for beamforming	19
2.6.2	Temporal $\Sigma\Delta$ modulation	20
2.6.3	Spatial $\Sigma\Delta$ modulation	20
2.6.4	Spatio-temporal $\Sigma\Delta$ modulation	21
3	Design	22
3.1	Simulation environment	22
3.1.1	Model description	22
3.1.2	Signals	23
3.1.3	The ADC designs	26
3.1.4	Selection of simulation parameters	27
3.1.5	Metrics	27
3.2	The simulations	28
3.2.1	SNR vs. angle for a single user	28
3.2.2	Spatial distinction	30
4	Results	32
4.1	Algebraic analysis of the $\Sigma\Delta$ modulators	32
4.1.1	Spatial $\Sigma\Delta$ modulator	32
4.1.2	Spatio-temporal $\Sigma\Delta$ modulator	32

4.2	Evaluation of reconstruction SNR vs. input power	33
4.2.1	Temporal $\Sigma\Delta$ modulation	33
4.2.2	Spatial $\Sigma\Delta$ modulation	34
4.2.3	Spatio-temporal $\Sigma\Delta$ modulation	35
4.3	Evaluation of reconstruction SNR vs. angle	36
4.3.1	Temporal $\Sigma\Delta$ modulation	37
4.3.2	Spatial $\Sigma\Delta$ modulation	39
4.3.3	Spatio-temporal $\Sigma\Delta$ modulation	43
4.4	Comparison	45
4.4.1	SNR comparison for low OSR	45
4.4.2	SNR comparison for high OSR	46
4.4.3	SNR trend	47
4.4.4	Bandwidth	47
4.5	Multi-user analysis	48
4.5.1	Temporal $\Sigma\Delta$ modulation	49
4.5.2	Spatial $\Sigma\Delta$ modulation	50
4.5.3	Spatio-temporal $\Sigma\Delta$ modulation	51
5	Discussion	52
5.1	Observations and findings	52
5.2	Limitations	53
5.3	Future work	54
6	Conclusion	55

Chapter 1

Introduction

A recent trend in digital wireless communication systems is to use several antennas at each end of a point-to-point connection. Current research focuses on very large arrays with hundreds of antennas. The large number of antennas allows for what is commonly referred to as beamforming, which can focus the signal intended for a certain user in the correct direction, for several users simultaneously [1]. Such antenna systems are currently being developed and evaluated for the coming 5G radio access networks [2]. In today's wireless communication systems, beamforming is not used, but multiple users are often scheduled in different frequency channels for communication in order to separate the signals. However, frequency spectrum licenses are very expensive and the spectrum available is decreasing due to an increasing number of wireless applications. By using beamforming in the system, users can be efficiently multiplexed in the spatial domain, while still using the same time-frequency resource.

Implementation of the multi-antenna systems necessary to perform beamforming poses several challenging problems, among which the following can be found: Consider, for instance, a 100-antenna system where each receiver samples the signal with one gigasample per second (1GS/s), and quantizes it with a resolution of 6 bits. The total digital bandwidth required from the receivers to the back end is then 600Gbit/s, which is difficult and expensive to handle (in [3] a 20 nm transceiver FPGA receives data at around 200Gbit/s). Thus, methods to reduce this bandwidth requirement are of considerable interest in order to reduce the overall power consumption and complexity. In [4], multi-antenna array systems are reviewed, and the benefits of such systems are made clear. However it is clear that multiple problems with current signal processing in such systems are present, for instance regarding required processing power. It is stated that the development of efficient signal processing of signals from such a system is motivated. The overall goal of this master thesis project is to reduce the required bandwidth and computational power in systems using antenna arrays. We investigate the use of the spatial dimension as part of a $\Sigma\Delta$ modulator to achieve this.

$\Sigma\Delta$ modulator Analog-to-Digital Converters (ADCs) have multiple benefits. Smaller CMOS processes allow higher speeds, but also leads to worse component inaccuracies. Thus, speed is improved at the cost of component inaccuracies. In a system consisting of potentially hundreds of ADCs working together, like the one in question, converter

uniformity is important. This is difficult to provide in high-resolution multi-bit Nyquist converters implemented in CMOS integrated circuits (ICs). One way to overcome this problem is to trade off speed for accuracy, which is done by the $\Sigma\Delta$ modulator since they are insensitive to nonideal component properties [5]. Another problem is also the power consumption and cost related with using many antennas and ADCs. $\Sigma\Delta$ modulators allow for cheaper and more reliable systems due to the absence of need to trim components and implementability on integrated circuits [6–8]. Since the higher speeds allow for high-resolution beamforming using simple hardware, $\Sigma\Delta$ modulators are favorable in beamforming applications in particular [9].

One drawback with using $\Sigma\Delta$ modulators is the increase in converter sampling rate. This motivates the interest in use of spatial $\Sigma\Delta$ modulation [7], to reduce the required oversampling ratio or perhaps eliminate the need for temporal oversampling altogether.

Some related work in this field has been carried out, but in other applications such as ultrasound and image processing. In [10], a method is described how to sample a picture using a 2-D $\Sigma\Delta$ modulator and utilize the correlation between adjacent pixels. In [11], a method is proposed where the beamforming is performed using delayed sample clocks in the different $\Sigma\Delta$ modulators in the array. In [12], a 2-D $\Sigma\Delta$ modulator design for an acoustical transducer array is proposed in which the spatial low-pass filtering eliminates the high frequency noise. Another approach where FIR-filters are used for beamforming is presented in [13]. Here, design principles for both narrowband and broadband signals are described. Furthermore, different algorithms such as optimum solution and less computation intensive calculations are discussed.

The strategy used throughout this master thesis project is to try to find an alternative modulator structure that can produce a higher SNR after beamforming and reconstruction filtering for a given sample rate than what a reference ADC could provide. More specifically, low sampling frequencies are of interest to keep the bandwidth low.

The fundamental deliverable of this master thesis project is an investigation of how the spatial dimension in $\Sigma\Delta$ modulation can be used to reduce the digital bandwidth required in an antenna array. One basic question to be answered is if the solutions actually works in a real system. Therefore, usability in a real environment and system is of focus.

Chapter 2

Theory

2.1 Wireless communication

Wireless communication in the context of modern cellular networks is done using fixed base stations and mobile users. The wireless link between them consists of a baseband signal with a certain bandwidth, up-converted to a certain carry frequency. Up-conversion is modulating the baseband signal with the carry frequency by multiplying the complex baseband signal with the carry frequency expressed as a complex exponential. Equation 2.1 shows this, if $s_b(t)$ is the baseband signal, $s(t)$ the modulated signal and f_c the carry frequency.

$$s(t) = \sqrt{2}\Re[s_b(t)e^{j2\pi f_c t}] \quad (2.1)$$

Multiplication in the time domain is convolution in the frequency domain, so the baseband signal is going to be moved up in frequency and centered around the carry frequency. With a baseband bandwidth W and a carry frequency f_c , the baseband signal is going to occupy $-\frac{W}{2}$ to $\frac{W}{2}$ centered around 0 in the frequency domain; after modulation it's going to occupy $f_c - \frac{W}{2}$ to $f_c + \frac{W}{2}$. In addition, taking the real part of the complex modulated signal will yield a complex conjugate mirrored image at corresponding negative frequencies. The effect of modulation and taking the real part can be seen in figure 2.1. At the receiver side the signal is demodulated by modulating with f_c again, and low-pass filtering [1].

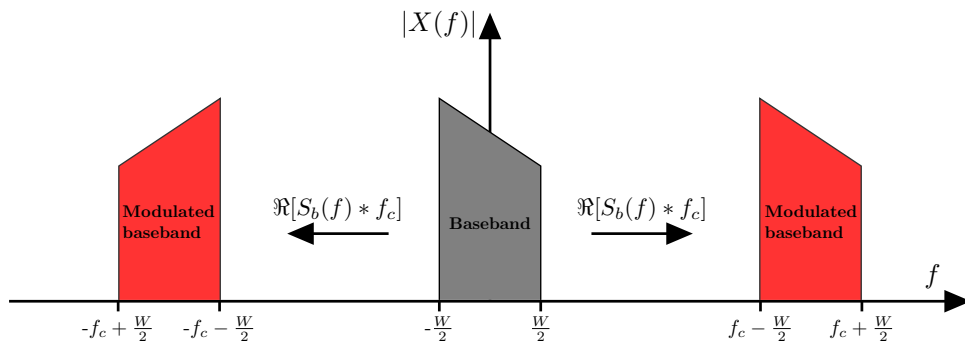


Figure 2.1: Modulation of a baseband signal

2.2 Beamforming

2.2.1 Principle

Beamforming, or spatial multiplexing, can be applied in several configurations such as Single Input Multiple Output (SIMO), Multiple Input Single Output (MISO), and Multiple Input Multiple Output (MIMO) channels [1]. SIMO has a setup of several transmit antennas and one receive antenna while MISO has a single transmit antenna and several receive antennas. A MIMO configuration consists of several transmit and receive antennas. They differ in the setup of the antenna array configurations depending on how the up-link and down-link are considered. Here, we consider the down-link case which means that a user transmits data with a single antenna to a receiving antenna array. In this master thesis, setups of MISO channels are evaluated in the base-station receiver only and spatial multiplexing for transmission is left out. The scenario is that a receiving antenna array listens simultaneously at multiple transmitting users, hence spatial multiplexing and this is depicted in figure 2.2. An important assumption is that there is a line-of-sight between the transmitters and receivers which is shown in the figure. The antenna separation distance is given by $\Delta_r \lambda_c$. The carrier wavelength is λ_c which is given by:

$$\lambda_c = \frac{c}{f_c} \quad (2.2)$$

where c is the speed of light and f_c is the RF-carrier frequency. The normalized receive antenna separation distance is denoted Δ_r which is normalized to the carrier wavelength. The value $\Delta_r = 1/2$ corresponds to half the carrier wavelength. The antenna array length is denoted L_r and computed as $L_r = n_r \Delta_r$, where n_r is the number of antenna elements. The parameters T_i , d_i and Θ_i describe the transmitting user, its distance to the antenna array center and its angle of incidence of the antenna array respectively.

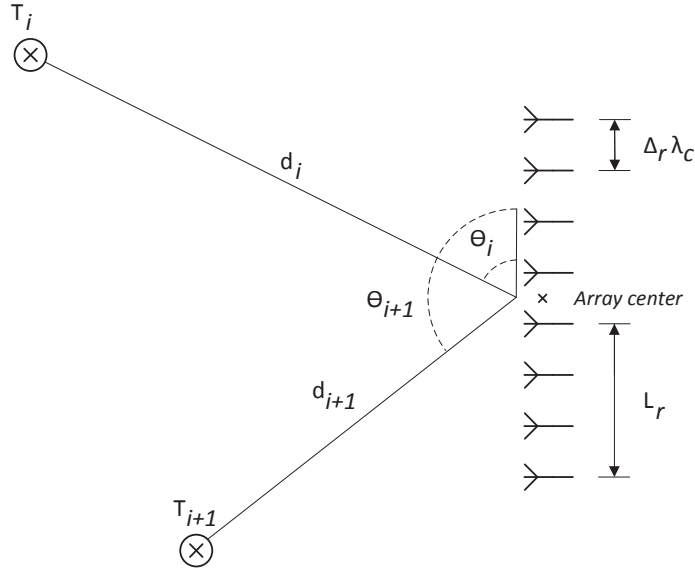


Figure 2.2: Configuration principle for the system evaluated in this project. This setup shows two different users that transmit data to a receiving antenna array. For each of the two users, this scenario corresponds to a MISO configuration in the down-link case.

It is possible to express the transformation between the spatial and angular domains. The angular domain is the inverse discrete Fourier transform of the spatially placed antenna elements. The discrete antenna array can be considered as a sampled continuous array. The incoming signal from a transmitting user is then a sampled version of the continuous spatial location. If the normalized antenna spacing is exactly $\Delta_r = 1/2$, this corresponds to temporal sampling with Nyquist frequency. This means that if the normalized antenna spacing is less than or equal to $1/2$, the sampled signal allows perfect reconstruction. The case when $\Delta_r > 1/2$ corresponds to undersampling which introduces aliasing Δ_r [1] [13] and will not be explored in this master thesis project. In the spatial domain this has the effect that the transmitting unit's location is erroneously interpreted.

In order to perform spatial multiplexing, information is required about the channel between the transmitting unit and the receive antenna array. Each transmitting unit sends a signal that arrives with a delay τ at each antenna element and this is referred to as the spatial signature. By adjusting for these incoming signal delays, the original signal can be combined constructively at the receiving antenna array [1] [13] by summation; as shown in figure 2.3. This enables the receive antenna array to listen to multiple transmitting units simultaneously; one user would need its own set of delay and summation. The antenna array is a phased array, and the principle of beamforming is a special case of Maximum Ratio Combining (MRC) [14]. In reality, the signal going the longest distance would have a weaker signal strength. This is however negligible since the antenna length is very small compared to the distance all signals are assumed to travel, and is therefore not considered at all.

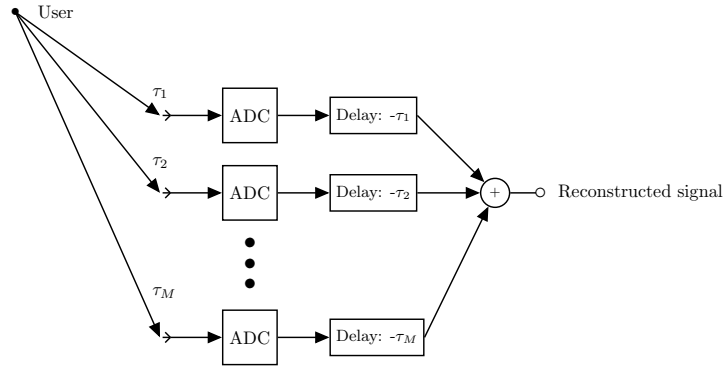


Figure 2.3: System model of the beamforming process

The result of sweeping the beamforming angle for a fixed positioned user can be seen in figure 2.4, which shows the received signal strength. The plots in figures 2.4 - 2.6 come from the beamforming simulator that was developed throughout this master thesis project. The results from these plots correspond to the responses described in literature [1], and this means that the plots here can be seen as a verification that the beamforming simulator works correctly. These plots are called the radiation pattern, or receive radiation pattern. Note that there is one pair of main lobes and several smaller side lobes. Since there are 8 receive antenna elements in this setup, there will be an amplitude gain of 8 after performing receive beamforming. The plots throughout figures 2.4 - 2.6 show the Root Mean Square (RMS)-value of the reconstructed signal after beamforming, normalized to one. Normally, the antennas are omni-directional which means that they receive signals from all directions between 0 and 360 ° but in these evaluations we only consider the range 0 to 180 °. This means that the values for the angles 181 to 360 in the plots correspond to mirrored values of the beamforming in the range 0 to 180 °.

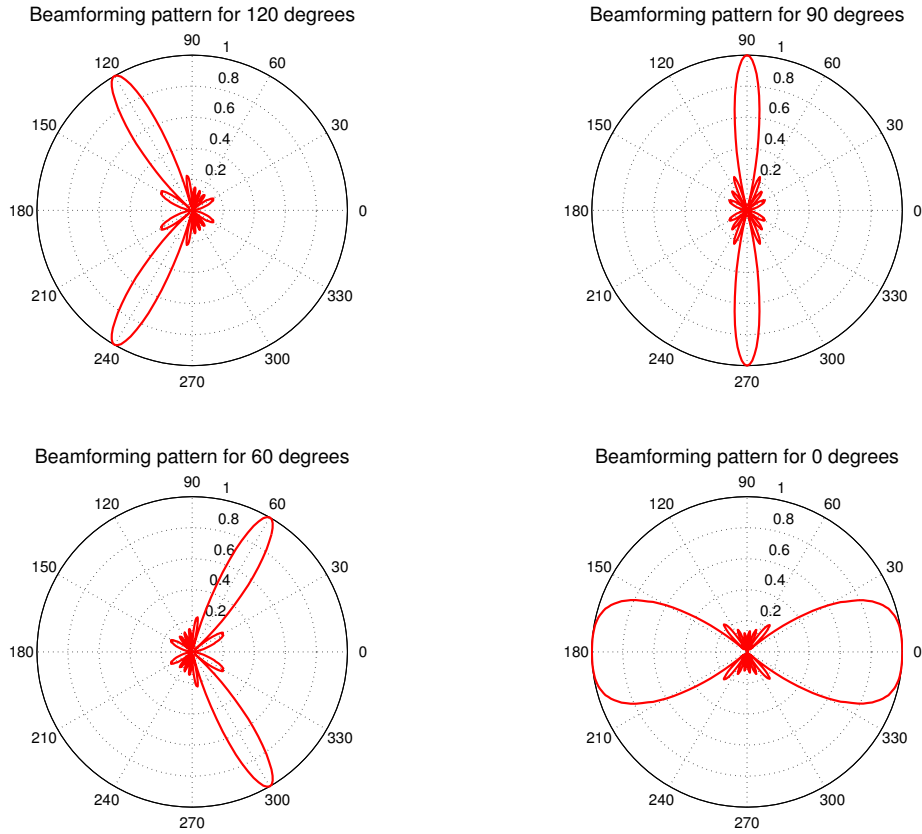


Figure 2.4: Radiation evaluated in the receiving angles of incidence for an array with $L_r = 4$, $n_r = 8$ and $\Delta_r = 1/2$. The transmitter signal is a 10 kHz sine wave with amplitude 0.8, on a distance of 20 m from the antenna array center. (a) angle 120° (b) angle 90° (c) angle 60° (d) angle 0° .

2.2.2 Spatial selectivity

A parameter that determines the beamforming quality is the antenna array length, L_r , which is related to the angular resolvability precision. The effect of three different antenna array lengths is shown in figure 2.5. From the figure it is clear that a longer antenna array makes the beam narrower which means that the array can distinguish a user with higher precision. The antenna separation is kept constant, and as such the number of antennas increase when L_r increases.

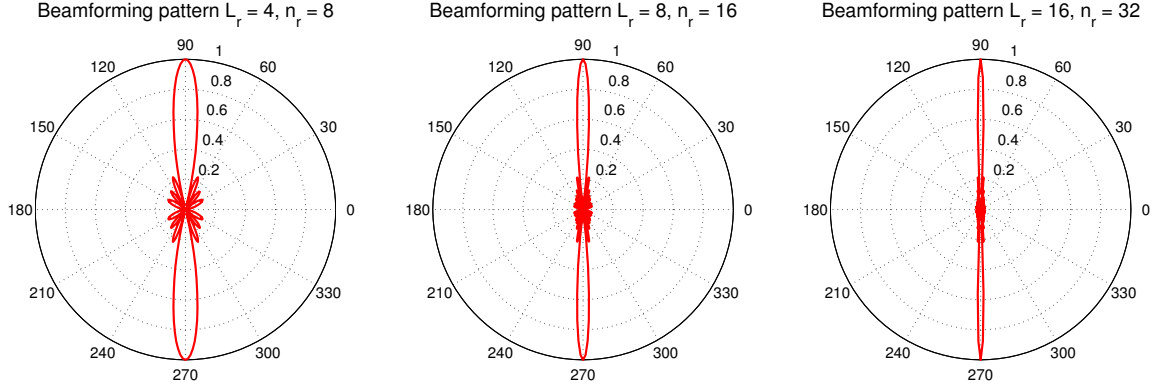


Figure 2.5: Radiation evaluated in the receiving antenna array lengths where $\Delta_r = 1/2$. The transmitter signal is a 10 kHz sine wave with amplitude 0.8, on a distance of 20 m from the antenna array center and with an angle of incidence of 90° . (a) $L_r = 4$, $n_r = 8$ (b) $L_r = 8$, $n_r = 16$ (c) $L_r = 16$, $n_r = 32$.

Another parameter that affects the beamforming is the normalized antenna separation distance, Δ_r . This parameter determines if there will be grating lobes in addition to the main lobes in the beamforming pattern. Grating lobes are similar to temporal undersampling, but in the spatial domain. Figure 2.6 shows the effect for three different normalized separation distances; $\Delta_r > 1/2$, $\Delta_r = 1/2$ and $\Delta_r < 1/2$. This time, the antenna array length is fixed and the number of antennas increase with smaller Δ_r to keep the length constant. In the first case, there is one main lobe pair and one grating lobe pair which means that the receive antenna array can not distinguish two users that are placed at the angles 60° and 120° ; a transmitting user that is placed at 120° will be erroneously detected at a listening angle of 60° . In the second case there is one main lobe pair. The last case also has one main lobe pair. One observation that can be made is that putting the antennas more densely does not add more precision in the intended beamforming direction but the sidelobes are reduced as a side effect.

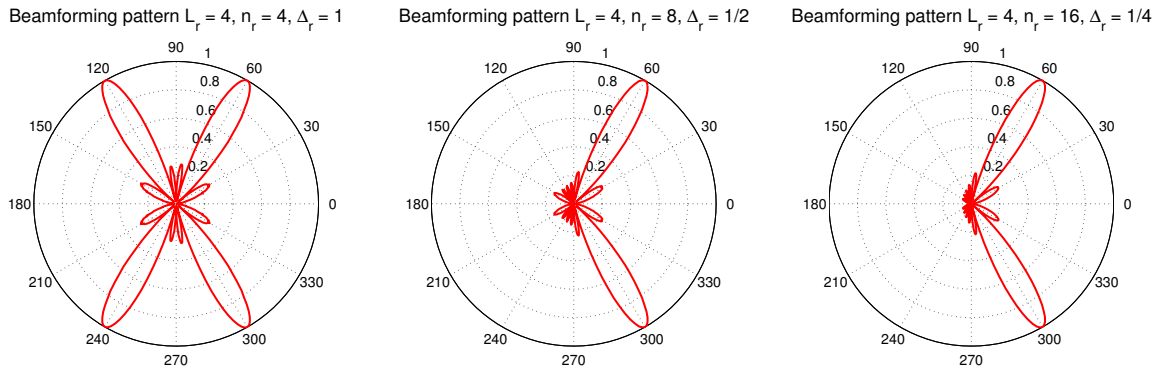


Figure 2.6: Radiation patterns for different normalized antenna separation distances where $L_r = 4$ is fixed. The transmitter signal is a 10 kHz sine wave with amplitude 0.8 and on a distance of 20 m from the antenna array center and with an angle of incidence of 60° . (a) $\Delta_r = 1$, $n_r = 4$ (b) $\Delta_r = 1/2$, $n_r = 8$ (c) $\Delta_r = 1/4$, $n_r = 16$.

The interpretation of the figures described above is that the receiving antenna array listens in a range of angles rather than one specific infinitely small angle. Thus, if two users are very close to each other, it is not possible to distinguish one from the other when performing beamforming. With this follows the requirement that the transmitter sources should be spatially placed in such a way that their signals do not interfere with each other at the receiving antenna array when beamforming to one of the users is done. From figure 2.2, this means that the two angles Θ_i and Θ_{i+1} should not be too close to each other.

2.3 The temporal $\Sigma\Delta$ modulator

2.3.1 Introduction

Oversampling techniques are used to achieve higher resolution and lower hardware requirements for conversion devices between the digital and analog domain. The $\Sigma\Delta$ modulator is such a system, which turns a signal with a large dynamic range into an oversampled signal with lower resolution. $\Sigma\Delta$ modulators are commonly used in ADC and DAC designs for reasons like insensitivity to component variations and implementability in integrated circuits due to the simple analog part [8].

2.3.2 System models

First-order $\Sigma\Delta$ modulator

A system model for a one-bit ADC utilizing a first-order $\Sigma\Delta$ modulator can be seen in figure 2.7. The resolution on the analog side is infinite, and it is to be converted to a bit-stream of two levels at some speed higher than the Nyquist frequency of the input signal. The difference between input signal X and output signal Y , the error, is integrated and quantized.

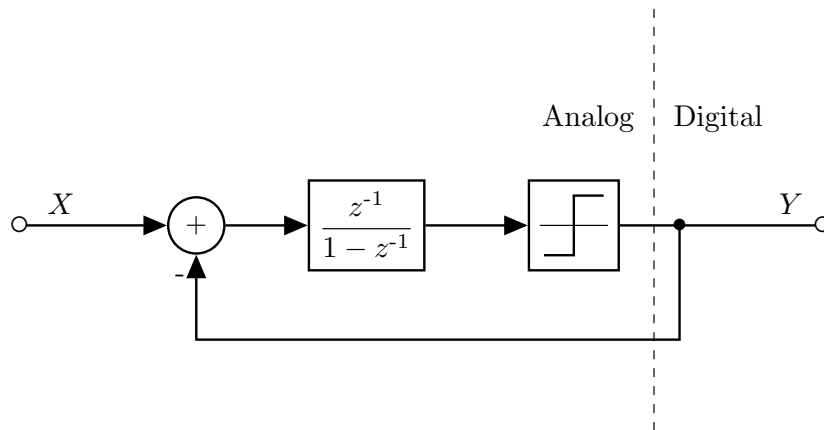


Figure 2.7: System of a first-order $\Sigma\Delta$ modulator

The quantizer block is non-linear since two different input levels to that block within the same range will produce the same output; this makes analysis quite hard. However, an equivalent linear system can be constructed by approximating the quantizer as an addition of white noise. This model is useful for analyzing the Signal Transfer Function (STF) and Noise Transfer Function (NTF), as well as the performance [8]. The equivalent linear model can be seen in figure 2.8, where Q is white noise.

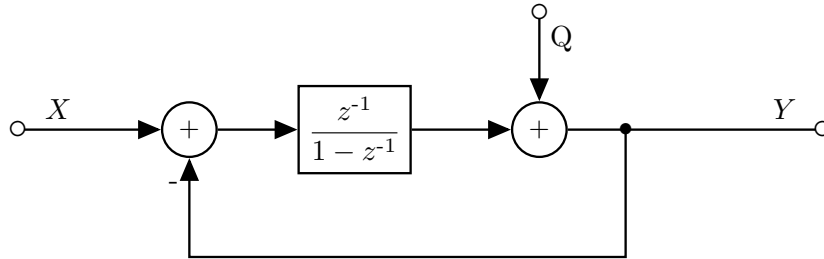


Figure 2.8: Linear system of a first-order $\Sigma\Delta$ modulator

Using the presented linear model, an expression for Y using X and Q can be formulated, making it possible to analyze what happens to the two input signals [15]. Equation 2.3 shows this.

$$Y(z) = X(z) \cdot z^{-1} + Q(z) \cdot (1 - z^{-1}) \quad (2.3)$$

Y is the sum of X with a delay, and a high-pass filtered Q . Since the signal is oversampled, X will exist somewhere in the lower part of the frequency spectrum, where the level of the noise is low. Y can then be low-pass filtered at half the Nyquist frequency of X to remove out-of-band noise, and then decimated to the Nyquist rate [15]. The expression for Y can also be expressed in terms of the NTF and STF, as shown in equation 2.4.

$$\begin{aligned} Y &= X(z) \cdot STF(z) + Q(z) \cdot NTF(z), \\ STF(z) &= z^{-1} \\ NTF(z) &= (1 - z^{-1}) \end{aligned} \quad (2.4)$$

In order to remove the delay on X , it is possible to formulate a similar model where the feedback is delayed rather than the input. The system model can be seen in figure 2.9.

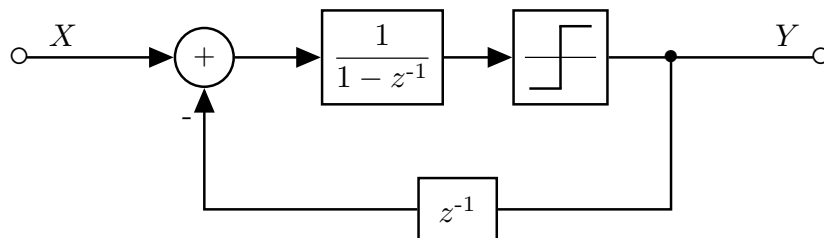


Figure 2.9: System of a first-order $\Sigma\Delta$ modulator without input-output delay.

We now get equation 2.5.

$$Y = (-Y \cdot z^{-1} + X) \cdot \frac{1}{1 - z^{-1}} + Q = \dots = X + Q \cdot (1 - z^{-1}) \quad (2.5)$$

An alternative equivalent implementation for the $\Sigma\Delta$ modulator is to feed back the negative error instead of the output; the system model can be seen in figure 2.10.

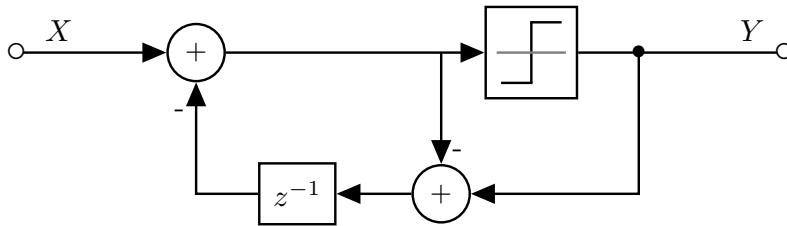


Figure 2.10: First-order $\Sigma\Delta$ modulator with error-feedback

Second-order $\Sigma\Delta$ modulator

There exists higher order $\Sigma\Delta$ modulators. The system model for a second-order $\Sigma\Delta$ modulator, using the error feedback design, can be seen in figure 2.11 [16].

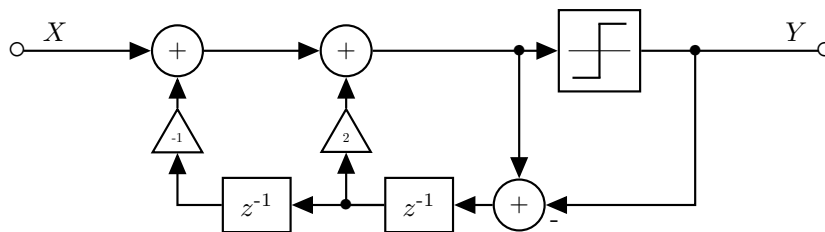


Figure 2.11: Second-order $\Sigma\Delta$ modulator with error-feedback

We get equation 2.6 [15]. The noise transfer function removes more noise from the band $[0 - f_b]$, increasing the Signal-to-Noise Ratio (SNR), but also causes there to be more noise outside of mentioned band which needs to be filtered.

$$Y = X + Q \cdot (1 - z^{-1})^2 \quad (2.6)$$

2.3.3 Mathematical expressions

OSR

For a certain signal with bandwidth f_b and Nyquist frequency $2f_b$ the Oversampling Ratio (OSR) is defined to be the number of times the signal is oversampled. For a sampling frequency f_s , the OSR is calculated according to [8]

$$OSR = \frac{f_s}{2 \cdot f_b} \quad (2.7)$$

First-order $\Sigma\Delta$ modulator

From the OSR and the number of bits n of the quantizer, it is possible to estimate the SNR of the frequency band $[0 - f_b]$. For a first-order $\Sigma\Delta$ modulator, the SNR can be estimated according to [15]

$$\text{SNR} = 6.02n + 1.78 - 5.17 + 9.03 \log_2(\text{OSR}) \quad (2.8)$$

It is obvious that the SNR improves when the OSR increases. Q is shaped by \sin^2 , which becomes more stretched out relative f_b as the OSR increases. This is shown in figure 2.12. The area between zero and f_b is the in-band noise power, and this area gets smaller as the OSR increases since the noise is pushed up higher in frequency by the noise-shaping function.

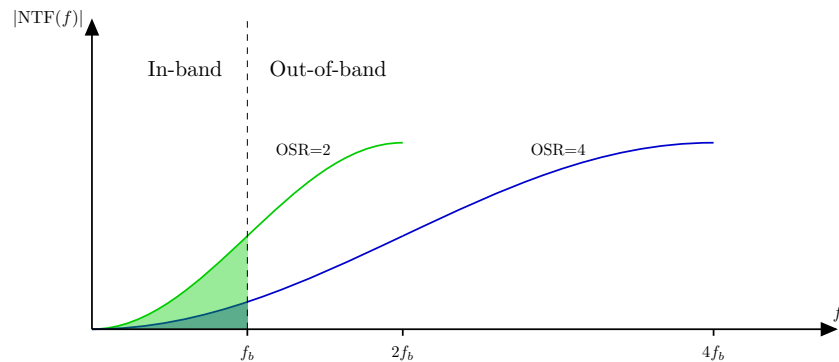


Figure 2.12: Frequency spectrum of the shaped noise

Second-order $\Sigma\Delta$ modulator

For a second-order $\Sigma\Delta$ modulator, the SNR of the frequency band $[0 - f_b]$ becomes equation 2.9 [15].

$$\text{SNR} = 6.02n + 1.78 - 12.9 + 15.05 \log_2(\text{OSR}) \quad (2.9)$$

2.3.4 Example

In a one-bit $\Sigma\Delta$ modulator, the output of a pure sine wave as input will be a pulse train of two levels where the average will be approximately equal to the input; this is commonly called pulse density modulation. Figure 2.13 shows the output of a first-order $\Sigma\Delta$ modulator in time domain.

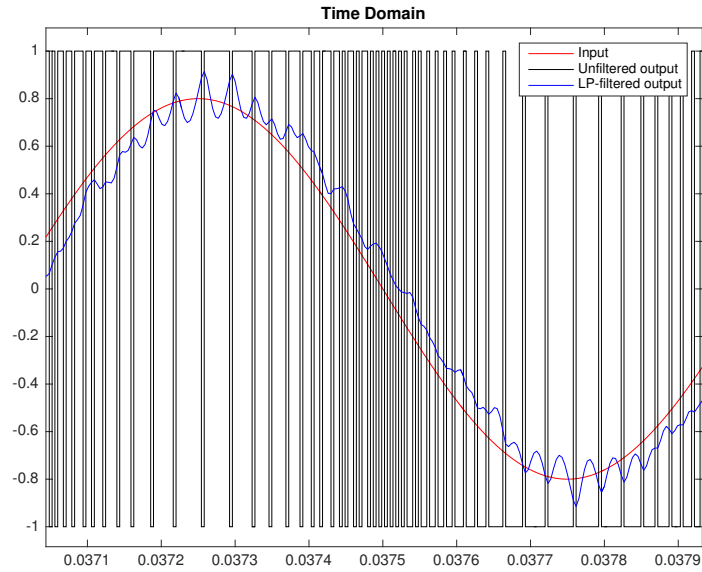


Figure 2.13: Output of a one-bit first-order $\Sigma\Delta$ modulator.

Figure 2.14 shows the frequency content; the high-pass character of the frequency domain of Q is obvious. The output is filtered at the Nyquist frequency to remove noise outside of the band of the input signal, which gives a signal closely resembling the input. The OSR was eight, and the SNR of the filtered output was 22.7 dB.

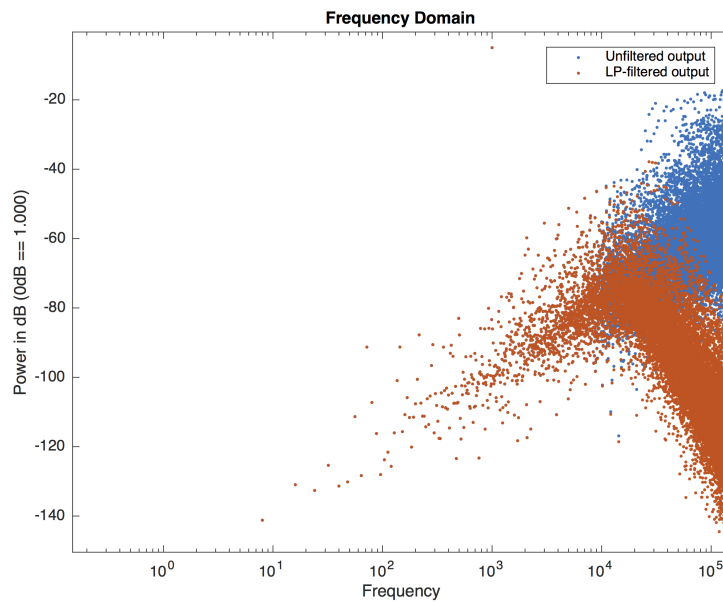


Figure 2.14: Frequency spectrum of the output of a one-bit first-order $\Sigma\Delta$ modulator.

2.4 The spatial $\Sigma\Delta$ modulator

2.4.1 Introduction

The connection between the temporal and spatial $\Sigma\Delta$ modulator is direct if time is exchanged by space. The Z-transform of a discrete time delay by one unit is z^{-1} . This means taking the previous sample in time. The equivalent function in space, a spatial delay, would mean going back in space rather than time. In other words, going back to the previous antenna for some direction. This also means that the integrator is no longer a time integrator but a space integrator. Perhaps needless to say, the spatial $\Sigma\Delta$ modulator is only applicable where there is a space; it wouldn't make much sense to apply such a system to a single transmit or receive antenna.

2.4.2 System models

The first-order $\Sigma\Delta$ modulator in figure 2.7 can be transformed into the system in figure 2.10, where the positive error from the previous quantization is subtracted from the input. This is perhaps the easiest model to start with in the spatial case. Using the reasoning about time-space equivalence, it's simply a matter of adding the quantization error from one antenna ADC to the next. The system model and its linear model can be seen in figure 2.15. Each input corresponds to the signal from one antenna in the array in figure 2.2.

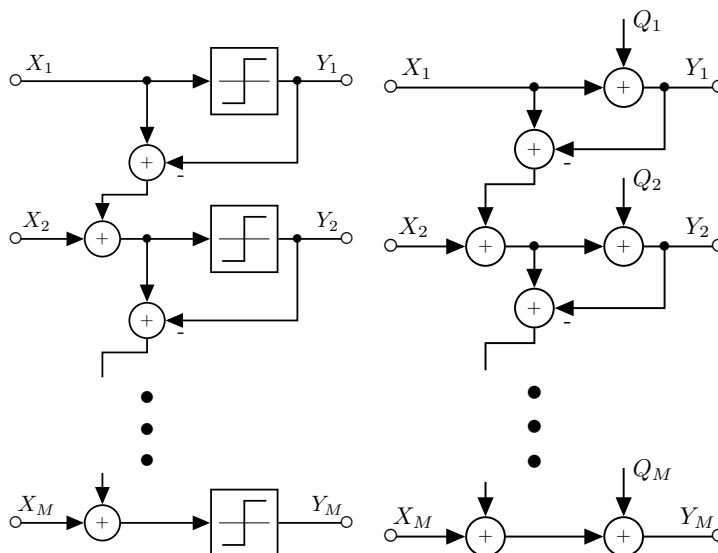


Figure 2.15: Left: System model for the spatial $\Sigma\Delta$ modulator. Right: Linear model.

2.4.3 Algebraic analysis

Looking at one ADC row, the spatial $\Sigma\Delta$ modulation doesn't make the quantization noise smaller at all. The benefit comes when they are summed, which is part of the beamforming

process. The negative error $-Q_{m-1}$ is added to the input of antenna m , and when the output signals are added the positive and negative errors will cancel out. If antenna m is assumed to have an ideal quantizer, and X_m and X_{m-1} are the same, this will look like the signals in figure 2.16, where the negative error from antenna $m-1$ is added to the input of antenna m and cancel out the error in the beamforming summation. Similarly, the error from the quantizer of antenna X_m , if there was one, would be corrected by antenna $m+1$ and so forth to the last antenna.

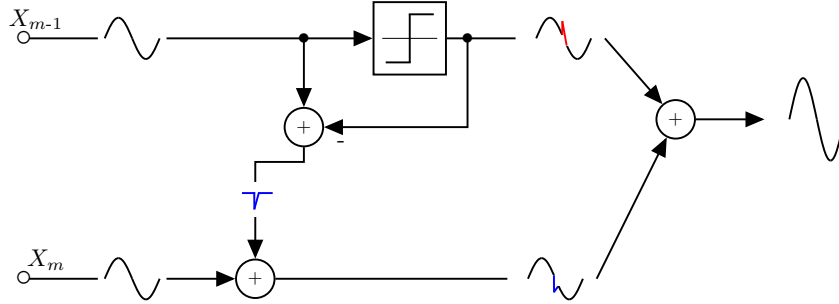


Figure 2.16: Signal path of a spatial $\Sigma\Delta$ modulator

Consider the system in figure 2.15 with M ADC rows, but with no spatial $\Sigma\Delta$ modulation, which means that the vertical connection from one ADC to another is left out. With Y_{sum} as the direct summation of all Y_1, \dots, Y_M , the following is true.

$$Y_{\text{sum}} = \sum_{m=1}^M X_m + \sum_{m=1}^M Q_m$$

Now, consider the unmodified systems in figure 2.15. The following is true.

$$Y_{\text{sum}} = \sum_{m=1}^M X_m + \sum_{m=1}^M Q_m - \sum_{m=1}^{M-1} Q_m = \sum_{m=1}^M X_m + Q_M$$

The only quantization error remaining is from the last ADC row.

However, this perfect cancellation of quantization errors is void if one Y is time delayed relative to its neighbor. Going back to the general system of a $\Sigma\Delta$ modulator in figure 2.10, whose behavior is still valid in the space dimension, Q is shaped by the function $(1 - z_1^{-1})$ which has the shape of a high-pass filter [12]. This implies that the spatial noise is mostly present at high spatial frequencies. Spatial frequency is the number of periods of a continuous signal per distance. The SI unit is cycles per meter. If the array is hit by a wave front from a transmitter at $\Theta = 90^\circ$ located very far away, the signal is going to reach each antenna element approximately simultaneously; the relative change antenna to antenna in one moment in time is zero. The largest change antenna-to-antenna in one time instant is when the transmitter is at $\Theta = 0^\circ$. To conclude, high spatial frequency implies large angles relative straight forward. As such, there will be little noise at low temporal frequencies which is straight in front of the array.

Following the reasoning above it can be stated that at angles far from $\Theta = 90^\circ$, the negative error is going to be skewed relative to the positive error due to the beamforming delay. This will make the resulting signal after beamforming best straight in front of the

array, and worse at angles off. Furthermore, since equidistant antennas on a straight line in the room is equivalent with uniform sampling in time, spatial oversampling simply means that the antennas are spaced closer than half the wavelength of the highest frequency ($\Delta_r < 1/2$). On the other hand, closer spacing would require more antennas to keep the same antenna length, which is required to maintain the spatial selectivity.

2.4.4 Second-order spatial $\Sigma\Delta$ modulator

It is possible to construct a second-order spatial $\Sigma\Delta$ modulator out of the temporal second-order $\Sigma\Delta$ modulator. The NTF from the temporal second-order $\Sigma\Delta$ modulator has lower gain on low frequencies compared to the NTF of a first-order $\Sigma\Delta$ modulator; using the reasoning of time and space it is possible that a spatial second-order $\Sigma\Delta$ modulator would have the same impact on spatial frequencies. As such, the point of using a second-order design would not be to better the signal quality but to widen the range in which the signal quality is good. Using figure 2.11 and mentioned reasoning, we get the system model in figure 2.17.¹

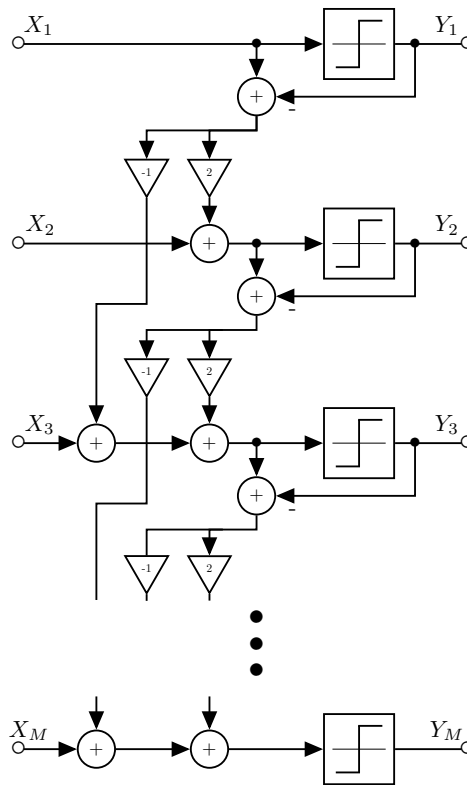


Figure 2.17: Second-order spatial $\Sigma\Delta$ modulator

¹The linear model is left out since arithmetic analysis is not considered.

2.5 The spatio-temporal $\Sigma\Delta$ modulator

It is possible to combine the temporal and spatial $\Sigma\Delta$ modulators to formulate a two-dimensional $\Sigma\Delta$ modulator. It can be implemented using two nested $\Sigma\Delta$ modulator loops, as seen in figure 2.18 [12, 17]. z_1 refers to the spatial dimension, and z_2 refers to the temporal dimension.

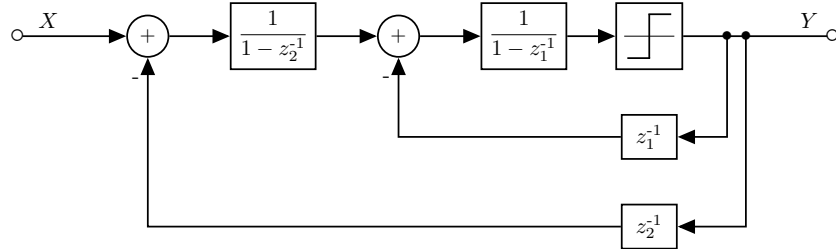


Figure 2.18: 2-D $\Sigma\Delta$ modulator

It is possible to derive an expression for the output Y in terms of X and Q , which can be seen in equation 2.10 [12]. Q refers to the added noise, which is modelling the quantizer.

$$Y = X + (1 - z_1^{-1})(1 - z_2^{-1})Q \quad (2.10)$$

Q is shaped by the function $(1 - z_1^{-1})(1 - z_2^{-1})$, which confirms the spatial and temporal noise shaping.

An implementation can be made by straight forward combining of the spatial and temporal $\Sigma\Delta$ modulator; figure 2.19 [12] [17].

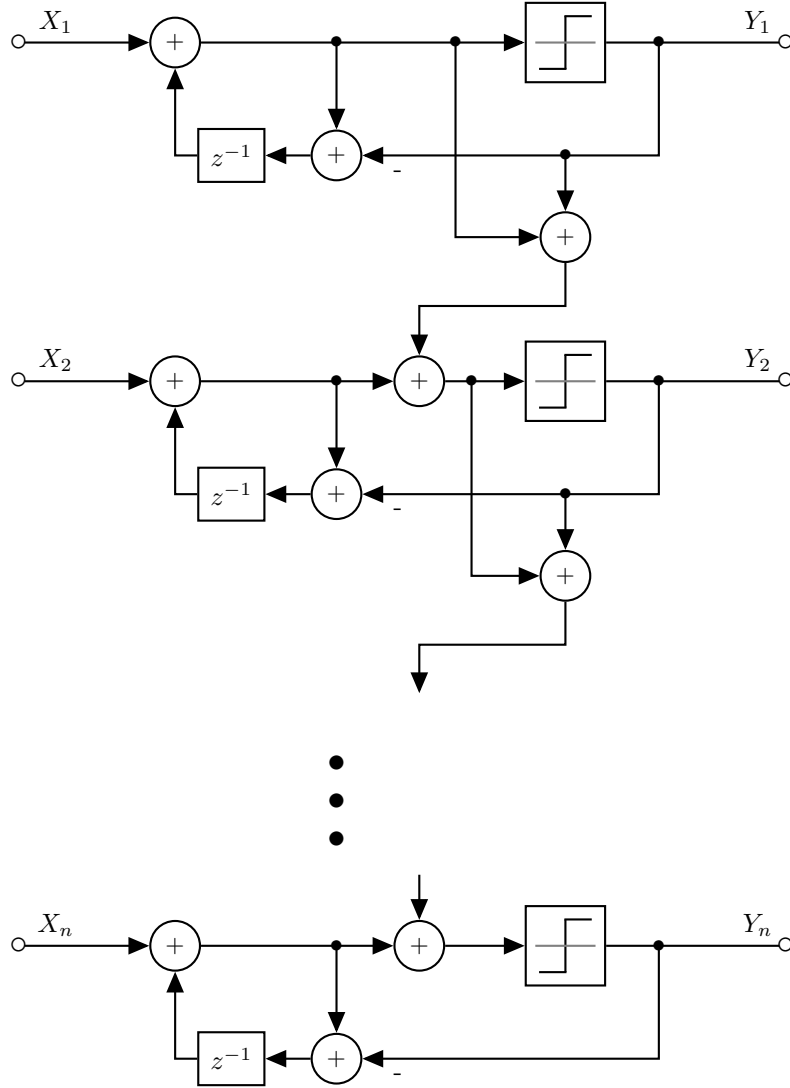


Figure 2.19: System model of a spatio-temporal $\Sigma\Delta$ modulator

2.6 $\Sigma\Delta$ modulation in a beamforming application

Thus far only the $\Sigma\Delta$ modulator designs outside of a beamforming system have been considered. It is however necessary to put them into the context of the system examined, which is a beamforming receive antenna. The impact that the beamforming operation has on SNR of the received signal is investigated, especially when beamforming in angles other than 90° . Finally, possible solutions are presented to solve the problems that arise. Algebraic analysis to analyze and verify them is presented in the Result chapter.

2.6.1 System model for beamforming

So far the inputs X_1, \dots, X_M in the system models have been assumed to be independent, but to be able to analyze how the ADCs behave in a beamforming array over a MISO channel (receive direction) it is necessary to define an equivalent baseband model with only one input and output so that the signal path can be analyzed. This requires a system model which takes the transmitter to antenna path, as well as the beamforming process, into consideration. In other words, it is desirable to exchange all X_1, \dots, X_M and Y_1, \dots, Y_M input signals for two signals: X and Y . Using the first hit of the transmitted signal X at any antenna as time reference and adding different delays on the inputs matching the relative propagation delays with respect to the time reference, it is possible to formulate a system model with only the transmitter signal as input. If the beamforming process is modeled using delays and a sum, there is only one output. Such system model could look like the one in figure 2.20.

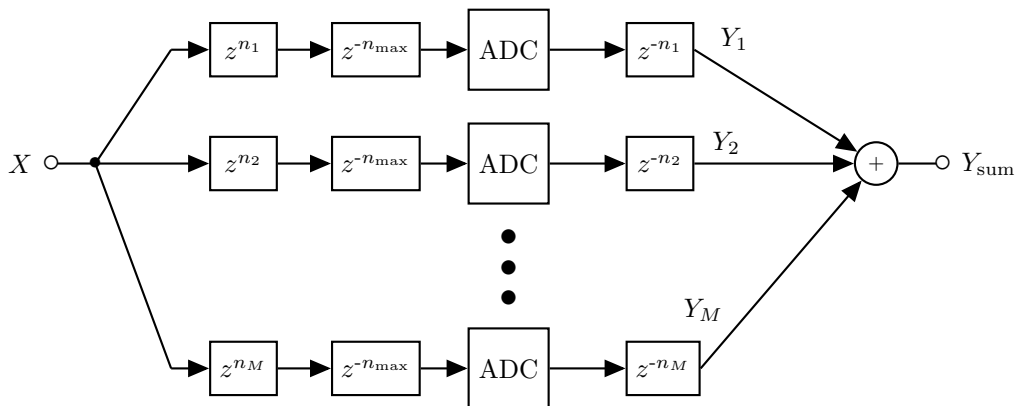


Figure 2.20: System model for modelling the channel and beamforming

n_{\max} is defined to be the largest delay of the spatial signature in samples, with respect to the time reference; in other words, the difference between the first and last hit of the signal for any antenna in the receive array. The delay blocks on the inputs, z^{n_m} where $m \leq M$, represents the propagation delay of the signal relative the time reference; the delay block of the antenna representing the time reference will be z^0 . Obviously if the transmitter is at an angle it is true that $n_m > 0$ for some $m \leq M$ since the signal will hit some antennas later than the time reference. Another block is added which delays the inputs n_{\max} number of samples, guaranteeing the causality of the system since it is never true that $n_m > n_{\max}$ for any m . The system in 2.20 can however be argued to be locally non casual, so the two blocks on the input are combined, forming the causal system in figure 2.21.

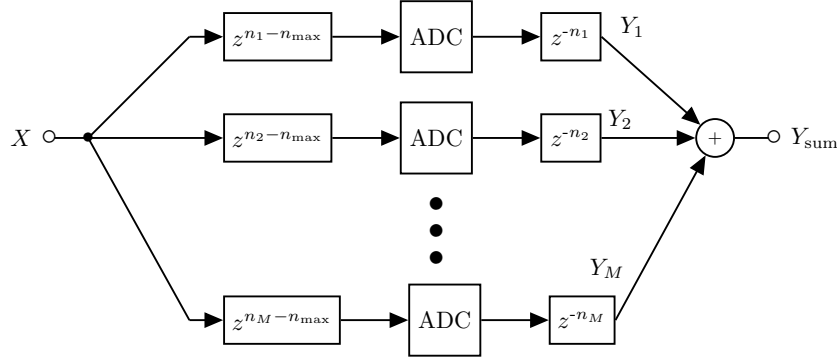


Figure 2.21: Casual system model for modelling propagation delay and beamforming

The delay on the outputs is to align the signals received before the time reference, to the time reference; this is the beamforming.

Assuming ideal ADC, Y_{sum} is the sum of the rows and thus

$$Y_{\text{sum}} = \sum_{m=1}^M X z^{n_m - n_{\text{max}}} z^{-n_m} = M X z^{-n_{\text{max}}}$$

Y_{sum} is a delayed sum of all the received X 's.

2.6.2 Temporal $\Sigma\Delta$ modulation

Using temporal $\Sigma\Delta$ modulation is not a problem in a beamforming application since the ADCs are operating entirely independently. There is no impact on the signal restoration quality when the user is placed at angles that deviate from 90 degrees.

2.6.3 Spatial $\Sigma\Delta$ modulation

It has been concluded previously that the spatial $\Sigma\Delta$ modulator in its original form only gives good performance when aiming the beam straight in front of the antenna very far away, in which case the delays on Y is very similar. It is however possible to move this point by inserting time delay in the error forward connection to compensate for the delays imposed on Y by the beamformer. This is the delay difference between two adjacent beamforming delays which can be formulated as $z^{\alpha_{m-1} - \alpha_m}$, where $z^{\alpha_{m-1}}$ and z^{α_m} denotes the delay imposed by the beamformer on antenna $m - 1$ and m respectively. It is only relevant for one beamforming direction. Inserting the beamformer delays from figure 2.20 into mentioned formula, the delay to be inserted in the error forwarding connection is $z^{-n_{m-1} - (-n_m)} = z^{n_m - n_{m-1}}$.

Figure 2.22 shows the proposed system and its accompanying linear model. The delays on the inputs represent the natural propagation delays, which is undone by the digital delays on Y . All z refer to the time dimension.

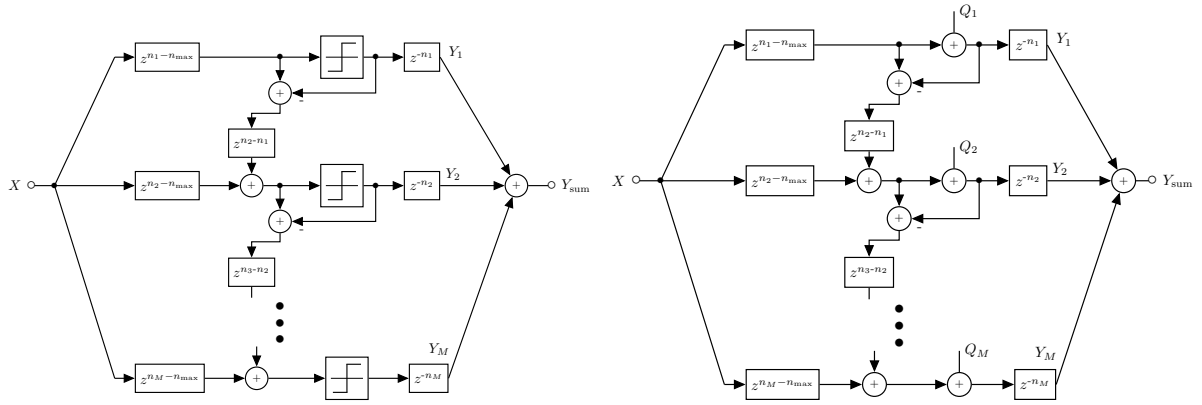


Figure 2.22: Left: System model for delay compensation in the error forwarding connection in a spatial $\Sigma\Delta$ modulator. Right: Linear model

2.6.4 Spatio-temporal $\Sigma\Delta$ modulation

As in the spatial $\Sigma\Delta$ modulator, it is possible to move the spatial position of the minima of the quantization error by delaying the error forwarding connection. The system model for such design, together with its linear model, is shown in figure 2.23

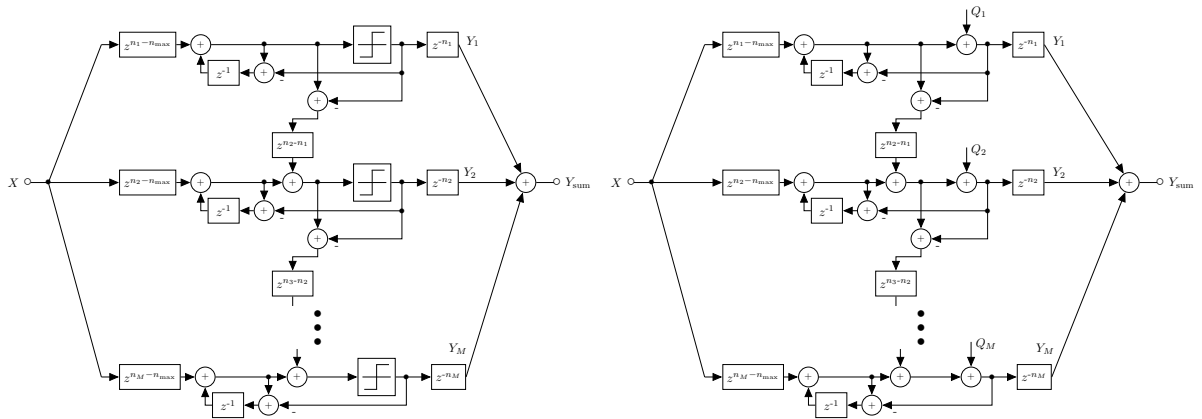


Figure 2.23: Left: System model for delay compensation in the error forwarding connection in a spatio-temporal $\Sigma\Delta$ modulator. Right: Linear model

Chapter 3

Design

3.1 Simulation environment

In order to be able to examine different ADC techniques in combination with beamforming, a simulation environment based on MATLAB and Simulink was developed. This enables evaluation of new ADC designs as well as comparison to existing conventional ADC designs. Only a straight one-dimensional array is considered.

3.1.1 Model description

In the simulation environment, we have modeled the wireless communication system as a system of sound propagation. Obviously, it would also be possible to set up a system very much like a communication system using electromagnetic radiation, or general system using only relative values.

In our simulation model, the critical antenna spacing is computed as $c_{\text{sound}}/(2f_c)$, and it is assumed that the signals transmitted from the user sources to the antenna array have the velocity c_{sound} . The basic idea is that trigonometry is used to calculate the distance from a given user position to each of the antenna elements. An example of a system configuration is given in figure 3.1. This distance is then converted to an equivalent delay based on sound propagation. The delayed versions of the user signal are then added on each of the antenna elements, emulating superposition when more than one user source is present. The signal delay at the topmost antenna, which is closest to the user, is calculated first and the delay at the bottom antenna is calculated last in an iterative manner.

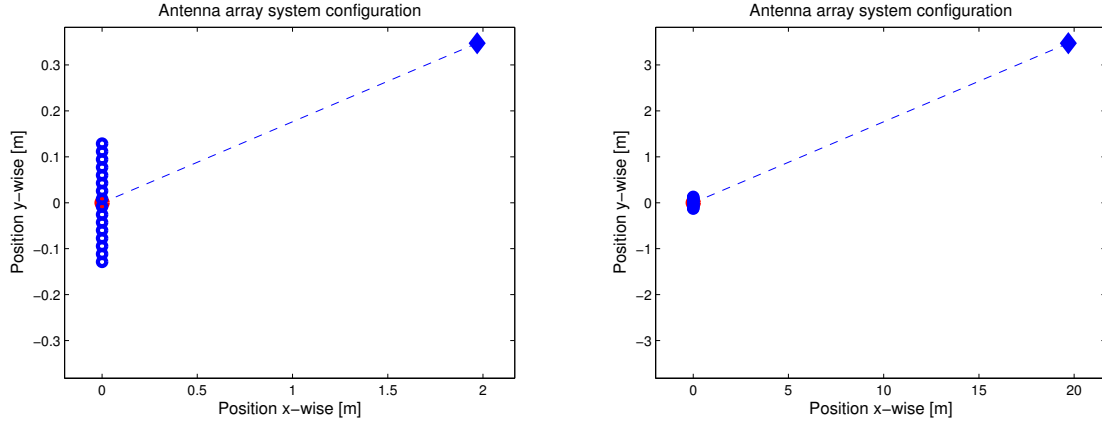


Figure 3.1: Example of antenna array system configuration with an angle of incident of 80° and 16 antennas. Note that the antenna array size appears to be very small as the distance gets larger. (a) User distance 2 m (b) user distance 20 m

The simulation model is able to simulate a custom amount of users for which settings of signal frequencies, distance from user source to antenna array center and angles of incidence are available. This makes it possible to set up a system configuration of several users and to evaluate the spatial distinction between them. Besides this, there are several adjustable parameters such as temporal sampling frequency, antenna spacing distance (spatial sampling), number of antenna elements and different ways to set the signal amplitude.

After the signal at each antenna has been calculated based on the simulation parameters, it is input to the ADC that is to be evaluated. The ADC is implemented in Simulink. The final stage is to do the beamforming in order to undo the delay which was imposed on the input; in other words to aim the beam. This is done by summing the delayed versions of each antenna element, based on the known signal delay that each user causes for each antenna element.

3.1.2 Signals

Input signal

In order to simulate a realistic wireless communication link, the transmitter user signal is bandlimited white noise which is similar to a modulated baseband signal. Our simulations are at low frequencies compared to a real system so a fair translation from a cellular system to our system of sound propagation is needed. The important property to keep is the ratio between the highest and lowest frequencies in a realistic wireless system. Thus, a bandwidth for our simulator can be calculated for a selected carry frequency. Equation 3.1 needs to hold, if f_{al} and f_{ah} is the low and high band limits respectively of our simulation, and f_{bl} and f_{bh} is the low and high band limits respectively of the real case.

$$\frac{f_{al}}{f_{ah}} \approx \frac{f_{bl}}{f_{bh}} \quad (3.1)$$

The 4G LTE standard was used as reference system. Multiple frequency bands are in use, from 450 MHz to 2.6 GHz; the most commonly used in commercially deployed systems being 1.8 GHz [18]. This frequency was selected to represent the real case which, seen from a logarithmic point of view, is quite close to the middle of the span. Bandwidths from 1.4 MHz to 20 MHz are supported [19]; 20 MHz was chosen since it represents the high-speed case. 10 kHz was selected as the carry frequency in the simulations, which using equation 3.1 gives a bandwidth of about 110 Hz. Thus, the transmitter signal occupies the frequency band 9945 Hz to 10055 Hz when being modulated.

The bandlimited noise signal was created by generating white noise in time domain and applying an ideal brickwall filter in the frequency domain; in other words, zeroing all frequency points outside the specified interval. The resulting signal was normalized to 1.0, and scaled according to desired peak signal amplitude. The number of sample points can be set; a larger number of sample points will yield a better filtering resolution. The power spectral density of the generated user signal can be seen in figure 3.2.

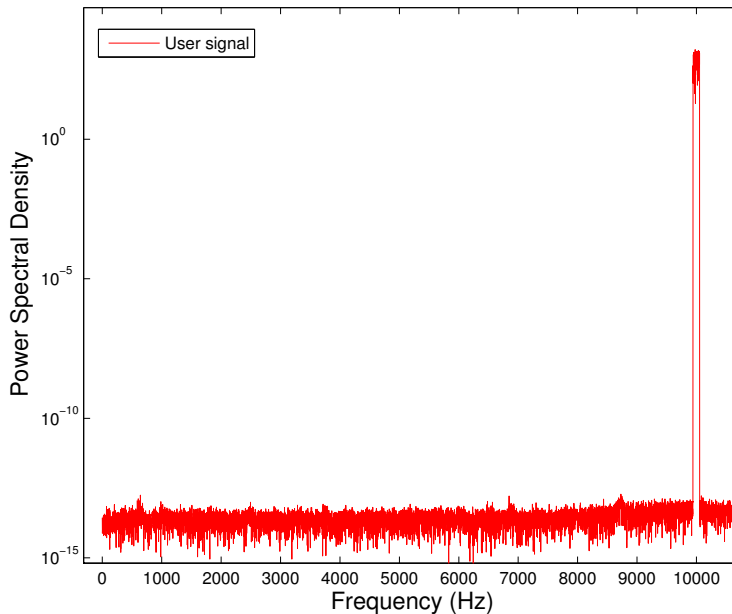


Figure 3.2: Power spectral density of user signal in simulator

The user signal amplitudes were designed such that the peak input amplitude to one antenna element would never exceed 0.8; if there are two users they would transmit maximum 0.4 in amplitude each. The reason for the choice of maximum signal amplitude of 0.8 was to avoid distortion in case noise is required to be added to the signal (to simulate antenna noise). Since distortion is caused by clipping in the quantizer at amplitudes close to 1.0, we chose to use a safety margin in order to avoid such effects.

In other words, all users (if more than one) were assigned equal signal strength. The motivation for this is that the focus lies on how signals (of equal strength) are reconstructed in different angles rather than simulating a realistic setup in terms of wireless communication. Having the same signal strength shows if there is an impact of the angle in a direct way; two or more users are reconstructed differently. Theoretically, the simulator

allows other choices of amplitudes to be made for the user signals, for instance assigning one signal twice as high amplitude as another.

The SNR vs input power relative to the full-range signal was evaluated for the case of a single ADC. The result of this evaluation is presented in figure 3.3. The single ADC is a temporal $\Sigma\Delta$ modulator that makes use of temporal noise shaping. As can be seen in the figure, the SNR increases for input amplitudes up to 1.0, after that the quantizer causes clipping of the signal which degrades the SNR.

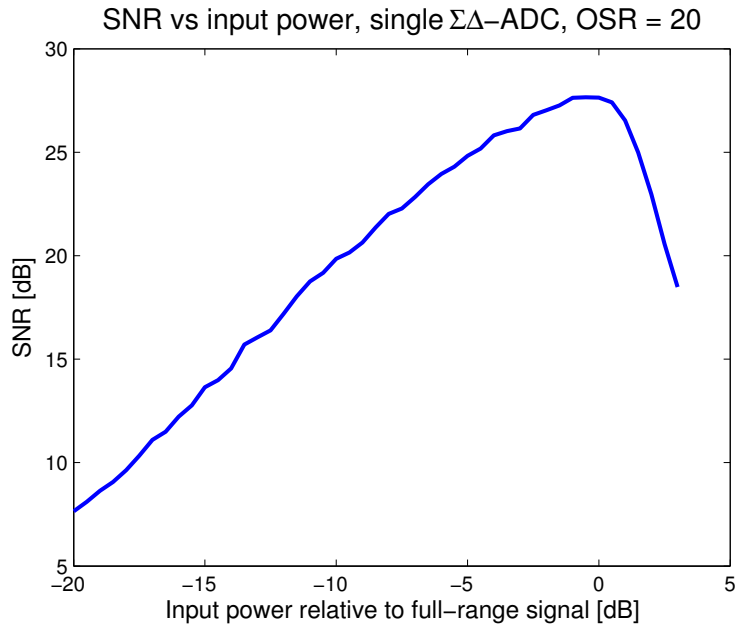


Figure 3.3: SNR vs input power relative to the full-range signal power for a single ADC. Temporal OSR = 20, the input signal is bandlimited white noise, dither power is -37 dB relative to the signal power. The data used to generate the plot is averaged over 100 signal realizations.

Dither

There is also a possibility to add white noise at each antenna element in order to improve the uncorrelation of the quantization noises from the different antennas. This is called dither. It is also possible to state that this represents a more realistic case since there is always noise in analog circuitry and antenna reception. Noise is required to give a fair comparison for the SNR in the case where the temporal $\Sigma\Delta$ modulator is used. As seen in figures 4.4 a - c, there is no SNR gain when the number of antenna elements increases. When noise is applied, as in figures 4.5 a - c, the antenna gain effect is present. The reason for this is that when no additional noise is applied, the quantization noise of all antennas is going to be exactly the same and the noise is going to increase with the same speed as the received signal, effectively keeping the SNR constant. If there is dither added it breaks up the correlation of the quantization noises from the different antennas and there will be addition of powers rather than addition of amplitudes, leading to a 3 dB increase per doubling rather than 6 dB as in the amplitude addition case.

The appropriate noise level was decided by trial. In order to have a starting point to be applied at each antenna, values from real applications were used as a reference. The noise power level was derived such that for a single full range ideal signal, the targeted SNR was around 25 dB since this is a common signal quality requirement for high speeds in wireless communication systems [20] [21]. A noise power level was chosen and simulations gave an SNR of around 24.7 dB for a single sine wave. However simulations showed that using the noise amplitude level described had a severely degrading impact on the spatial and spatio-temporal $\Sigma\Delta$ modulators. The maximum SNR when applying this noise level was reduced with between 10 to 15 dB. In order to find a compromise, the noise level was reduced until the antenna gain effect of the temporal $\Sigma\Delta$ modulator was considered acceptable while not influencing the maximum SNR for the spatial and spatio-temporal $\Sigma\Delta$ modulators too much. A suitable noise power level relative to the input signal power was determined to be

$$10 \log_{10}((\sqrt{0.001 \cdot 0.8})^2 \cdot \sigma_w^2) - 10 \log_{10}\left(\frac{0.8^2}{2}\right) \approx -37\text{dB}$$

where w is uniformly distributed random noise. This resulted in the SNR values in figure 4.5 a - c which were evaluated and the SNR improvement from 16 to 64 antennas had a mean value of 4.2 dB (theoretically 6 dB expected) while the SNR improvement from 64 to 128 dB was 2.8 dB (theoretically 3 dB expected). As can be seen from figure 4.14 and figure 4.13, there is no substantial SNR degradation for the spatio-temporal $\Sigma\Delta$ modulator when applying this reduced noise.

The noise power levels used in the simulations are thus, either no noise or -37 dB relative to the signal power.

3.1.3 The ADC designs

Apart from the proposed ADC designs that are evaluated here, an ideal multi-bit quantizer operating at the Nyquist frequency acts as a reference case. Each ADC design is a direct implementation of the system models presented. The inputs are calculated using the setup described, fed to the Simulink models, and each output is individually low-pass filtered at half the Nyquist frequency with a third-order Butterworth filter. Each ADC row is run separately from top to bottom, saving the output, and the error in the spatial case.

The multi-bit Nyquist ADC is implemented using a lookup table, without filtering the output. The Nyquist ADC system model is shown in figure 3.4. Instead of sampling it faster with a certain temporal OSR, the number of bits in the quantizer is increased accordingly. For instance, a Nyquist ADC with 2 bits is equivalent to a temporal OSR of 2 for the three $\Sigma\Delta$ modulators to be evaluated. Similarly, 8 bits in the Nyquist ADC corresponds to a temporal OSR of 8.

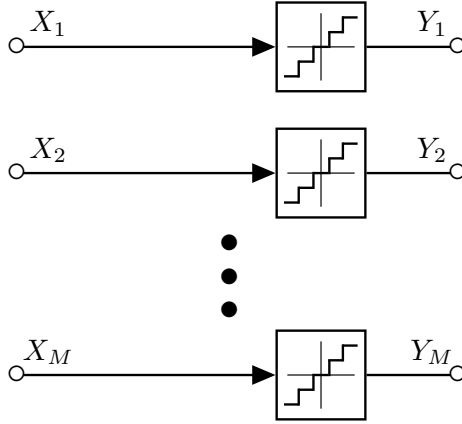


Figure 3.4: System model for the multibit Nyquist ADC

3.1.4 Selection of simulation parameters

There is an abundance of parameters and combinations that can be simulated. A set of discrete choices were selected. Three different antenna spacings have been used in the evaluations: $\frac{\lambda}{2}$, $\frac{\lambda}{10}$ and $\frac{\lambda}{20}$. These correspond to the critical antenna spacing distance as well as two arbitrarily chosen cases of spatially oversampled antenna spacings. Three different setups of number of antennas were selected to be 16, 64 and 128. It was assumed that a minimum number of antennas to be evaluated should be 10. The number of antennas were chosen as powers of 2, and since 16 is the first that exceeds 10, this was chosen as the lower value. The upper amount of the number of antennas, 128, was based on recent research [4] while 64 antennas was used as a value between the two extremes. A temporal OSR of 2 was chosen for the majority of the evaluations. Furthermore, a one-bit quantizer was selected for the $\Sigma\Delta$ modulators

3.1.5 Metrics

In order to evaluate the proposed $\Sigma\Delta$ modulation designs, we use two metrics. One of the parameters used is RMS. The RMS value in this context refers to the RMS value of the reconstructed user signal after the beamforming process in a certain direction. Thus, the RMS value shows the reconstructed signal strength rather than being a quality measurement. Figure 2.4 - 2.6 show examples of the signal strength in different beamforming directions.

The second metric is the SNR for a user signal after it has been reconstructed by the beamforming process in a certain angle. It is obtained by calculating the Normalized Mean-Square Error (NMSE). There exists two signals after beamforming reconstruction; one reference, and one estimated or reconstructed. The reference signal is compared to the reconstructed signal and the difference between these is considered as noise. Then the SNR is computed as the reference signal divided by the noise. NMSE is in fact the inverse of SNR; expressed in dB one is simply a negation of the other. For consistency we use the SNR quantity, but we calculate it using the NMSE. If \mathbf{x} and \mathbf{y} are vectors representing

the reference signal and estimate respectively, and α is a scalar to normalize \mathbf{y} to \mathbf{x} in order to remove constant gain and phase errors, the SNR can be calculated according to

$$\alpha = \frac{E(\mathbf{x}^H \mathbf{y})}{\sigma_y^2}$$

$$\text{SNR} = 10 \log_{10} \left(\frac{\sigma_y^2}{E(|\mathbf{x} - \alpha \mathbf{y}|^2)} \right)$$

The SNR value thus shows how accurately the user signal was reconstructed after the beamforming process, and is therefore a quality measurement.

3.2 The simulations

There are two distinct tests that can be performed by the beamforming simulator. One test is run to evaluate the SNR of the signal reconstruction for a single user as a function of the beamforming direction angle (which ranges from 0 to 180 degrees). The other test enables multiple users to be placed and evaluated.

3.2.1 SNR vs. angle for a single user

In order to determine the RMS and SNR values of the signal reconstructed in the beamforming direction as a function of the angle of incidence, it is possible to sweep the beamforming direction angle for a single user. For a constant distance from the antenna array center, the RMS and SNR values are evaluated for the user placed at each beam-angle that is swept with a given resolution, from 0 to 180°. The procedure is evaluated in figure 3.5. The red half circle in the figure indicates how to interpret the beamforming angle. Straight on top of the antenna, the angle is 0 degrees while straight down of the antenna array corresponds to 180 degrees. This red half circle corresponds to the range 0 to 180 degrees in the example plot shown in figure 3.6. This way, the SNR quality for a reconstructed single user signal can be evaluated as a function of the beamforming angle.

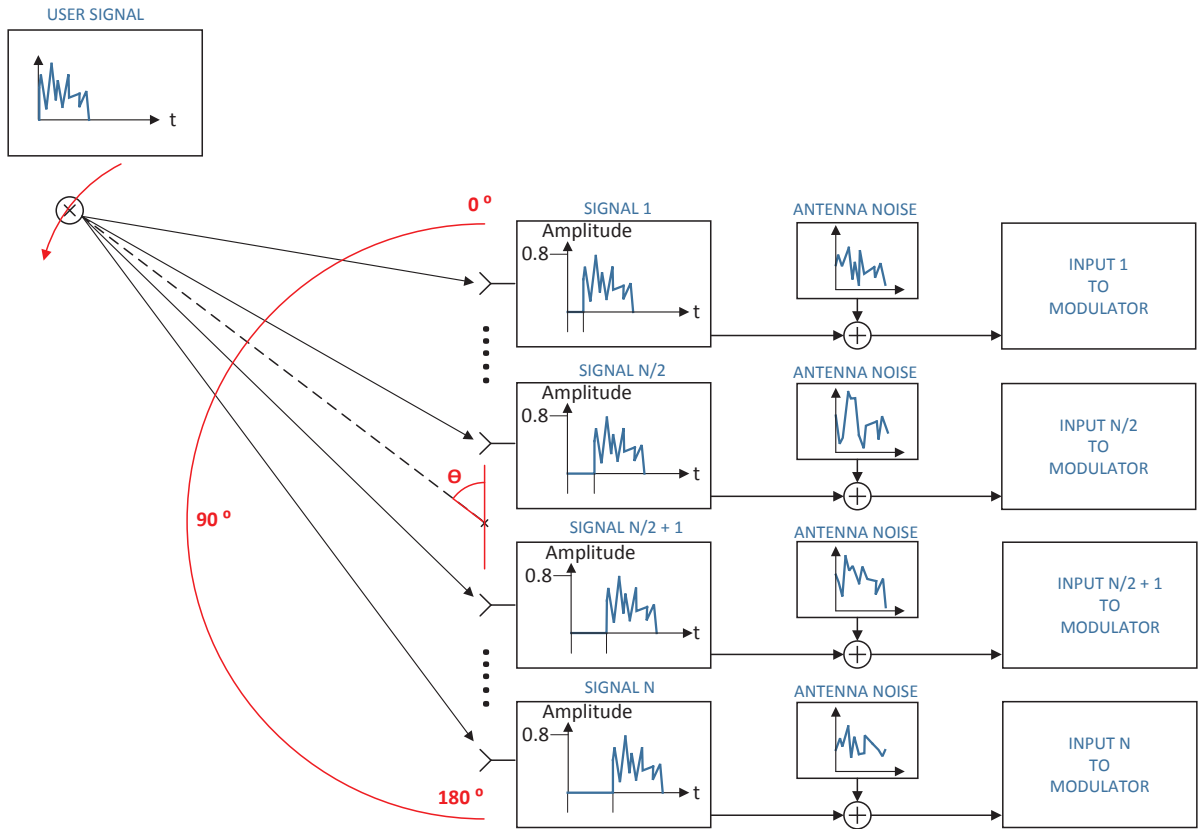


Figure 3.5: Principle of evaluating the SNR for a single user as a function of beamforming angle.

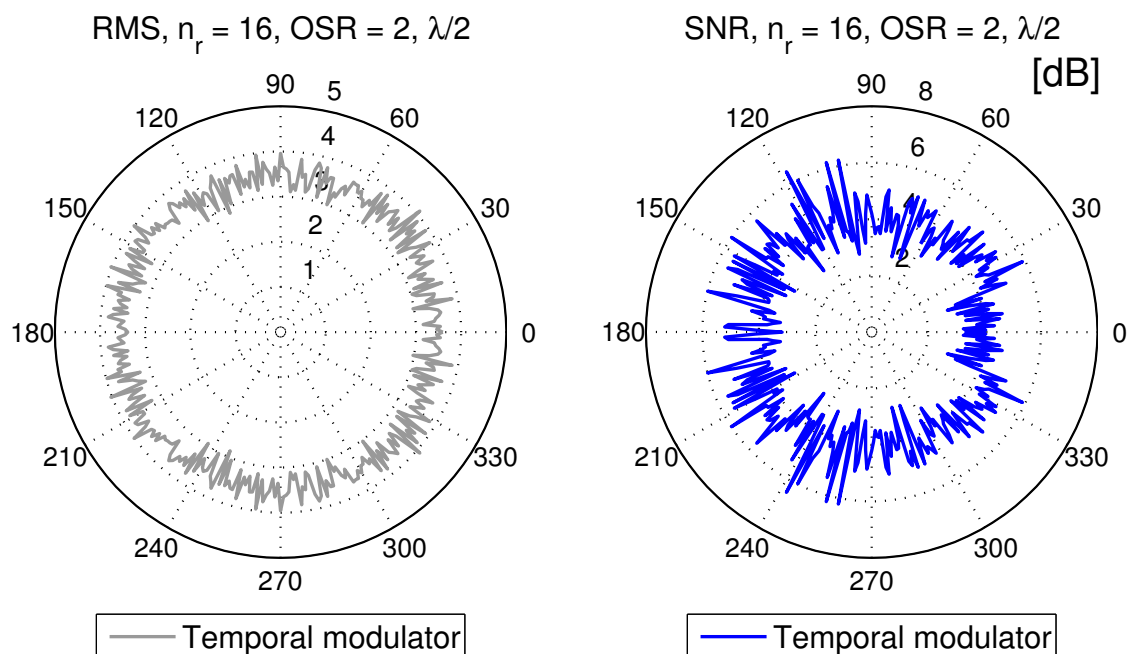


Figure 3.6: Example of the result from listening in angles 0 to 180° with an angle resolution of 1° with one user transmitting 20 m from the antenna array center. The modulator is of temporal type. The antenna spacing at the critical antenna spacing distance = $\lambda/2$, number of antennas = 16 and OSR = 2. Dither with power level = -37dB added. (a) RMS (b) SNR

3.2.2 Spatial distinction

In order to be able to evaluate the spatial distinction in a setup with multiple users, there exists a sweeping function for the beamforming angle. This is done by creating the superpositioned signal contributions at the antenna array, sweep the beamforming direction angle and calculate the RMS or SNR of the reconstructed signal.

Figure 3.7 shows an example of what such a plot might look like. The RMS plot shows the reconstructed signal content strength over the entire angle range in one plot. The SNR, however, is presented in a separate plot for each user. In this case, the spatial distinction is very good since the SNR width is very narrow and precise in the angles 80° and 35°, where the users are placed. The SNR values for the two users are different because the signals are generated randomly. As opposed to the sweep described in the previous subsection where a user is placed at each angle, this sweep listens in each angle with constant positions of the users.

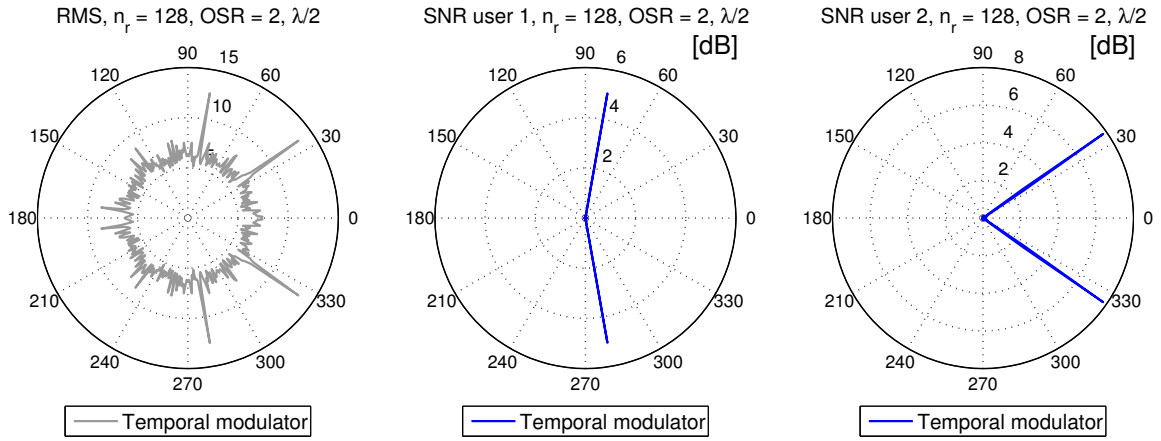


Figure 3.7: Example of the result from listening in angles 0 to 180° with an angle resolution of 1° with two users transmitting 20 m from the antenna array center and with angles of incidence of 80 and 35° respectively. The antenna spacing at the critical spacing distance $\Delta_r = 1/2$, number of antennas = 128 and OSR = 2. Signal amplitude 0.8/2 for each user. Dither with power level = -34dB relative to the input signal power. (a) RMS (b) SNR for user 1 (c) SNR for user 2

Chapter 4

Results

4.1 Algebraic analysis of the $\Sigma\Delta$ modulators

Algebraic analysis is done to examine the proposed solutions of the error and negative error skew problem that arise in the $\Sigma\Delta$ modulators using the spatial dimension. These solutions were presented in the Theory chapter.

4.1.1 Spatial $\Sigma\Delta$ modulator

Through algebraic analysis it is possible to verify that only the last quantization error remains. Let's consider system model 2.22 with M antennas but with no delay compensation in the error forwarding connection. In such system, equation 4.1 is valid.

$$Y_{\text{sum}} = MXz^{-n_{\text{max}}} + \sum_{m=1}^{M-1} [Q_m(z^{-n_{m-1}} - z^{-n_m})] + Q_M z^{-n_M} \quad (4.1)$$

If the transmitter is very far away straight in front of the antenna array, then $n_{m-1} = n_m$ for all m and thus all Q will cancel out except the last one. However if the transmitter is at an angle, the errors will remain. Now, let's consider figure 2.22 unmodified. Then, equation 4.2 is valid.

$$\begin{aligned} Y_{\text{sum}} &= MXz^{-n_{\text{max}}} + \sum_{m=1}^{M-1} [Q_m(z^{-n_{m-1}} - z^{n_m - n_{m-1}} z^{-n_m})] + Q_M z^{-n_M} \\ &= MXz^{-n_{\text{max}}} + Q_M z^{-n_M} \end{aligned} \quad (4.2)$$

Remaining is the received signal, but delayed, and the quantization noise from the last ADC row. The error has been shaped in space.

4.1.2 Spatio-temporal $\Sigma\Delta$ modulator

Again, let's consider the system model in figure 2.23 without the delay compensation in the error forwarding connection. In such system, the output can be calculated according

to equation 4.3

$$Y_{\text{sum}} = MXz^{-n_{\text{max}}} + \sum_{m=1}^{M-1} [Q_m(1 - z^{-1})(z^{-n_{m-1}} - z^{-n_m})] + Q_M(1 - z^{-1})z^{-n_M} \quad (4.3)$$

The quantization noise, except from the last ADC row, is cancelled out when the beamforming delays are equal. However if the beamforming angle is causing the digital delays to deviate from each other, the quantization noise will remain.

Considering the system model in figure 2.23 in full, the output can be found to be equation 4.4

$$\begin{aligned} Y_{\text{sum}} &= MXz^{-n_{\text{max}}} + \sum_{m=1}^{M-1} [Q_m(1 - z^{-1})(z^{-n_{m-1}} - z^{n_m - n_{m-1}} z^{-n_m})] + Q_M(1 - z^{-1})z^{-n_M} \\ &= MXz^{-n_{\text{max}}} + Q_M(1 - z^{-1})z^{-n_M} \end{aligned} \quad (4.4)$$

The received signal, delayed, as well as the noise-shaped quantization noise from the last ADC row is what remains.

4.2 Evaluation of reconstruction SNR vs. input power

Here, the reconstruction SNR is evaluated against input signal power expressed in dB. The evaluations are made for the three modulator structures for two different OSR cases; OSR = 2 and OSR = 20.

4.2.1 Temporal $\Sigma\Delta$ modulation

Figure 4.1 shows an evaluation of the reconstruction SNR vs input power relative to the full-range signal. It is obvious that the lower value of OSR does not cause the SNR to decrease when the input amplitude exceeds 1.0. The higher case of OSR clearly shows that the SNR decreases when the input amplitude exceeds 1.0.

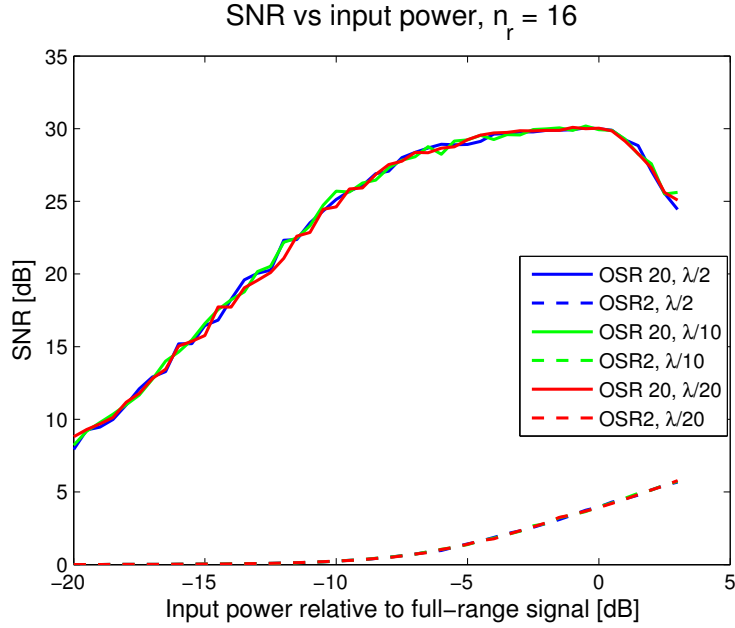


Figure 4.1: Reconstruction SNR vs. input power relative to full-range signal power for multiple ADCs in the context of beamforming for different antenna spacings and OSR. The input signal is bandlimited white noise, dither power is -37 dB relative to the signal power, number of antenna elements = 16, evaluation angle = 90 °. The results shown here are the mean values of 100 simulation runs for the temporal $\Sigma\Delta$ modulator.

4.2.2 Spatial $\Sigma\Delta$ modulation

Figure 4.2 shows an evaluation of the reconstruction SNR vs input power relative to the full-range signal. It is obvious that the lower value of OSR does not cause the SNR to decrease when the input amplitude exceeds 1.0. The higher case of OSR clearly shows that the SNR decreases when the input amplitude exceeds 1.0.

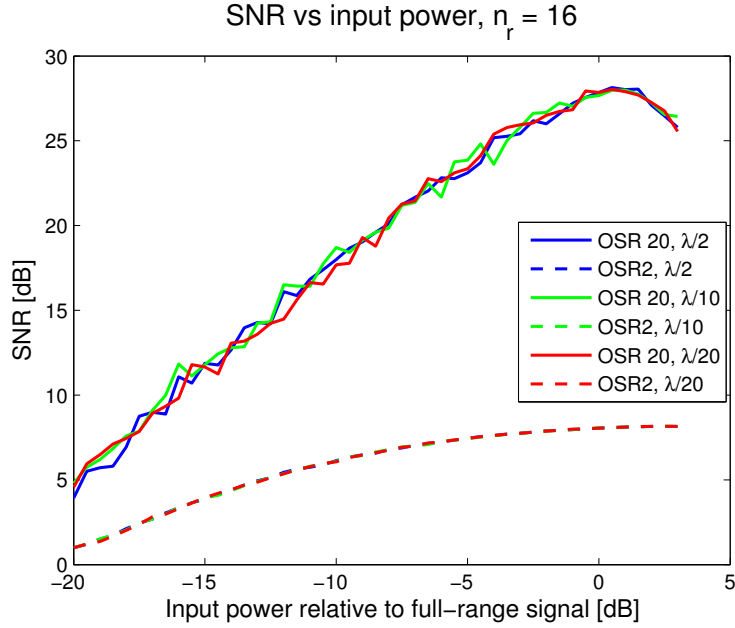


Figure 4.2: Reconstruction SNR vs. input power relative to full-range signal power for multiple ADCs in the context of beamforming for different antenna spacings and OSR. The input signal is bandlimited white noise, dither power is -37 dB relative to the signal power, number of antenna elements = 16, evaluation angle = 90 °. The results shown here are the mean values of 100 simulation runs for the spatial $\Sigma\Delta$ modulator.

4.2.3 Spatio-temporal $\Sigma\Delta$ modulation

Figure 4.3 shows an evaluation of the reconstruction SNR vs input power relative to the full-range signal. It is obvious that the lower value of OSR does not cause the SNR to decrease when the input amplitude exceeds 1.0. The higher case of OSR clearly shows that the SNR decreases when the input amplitude exceeds 1.0.

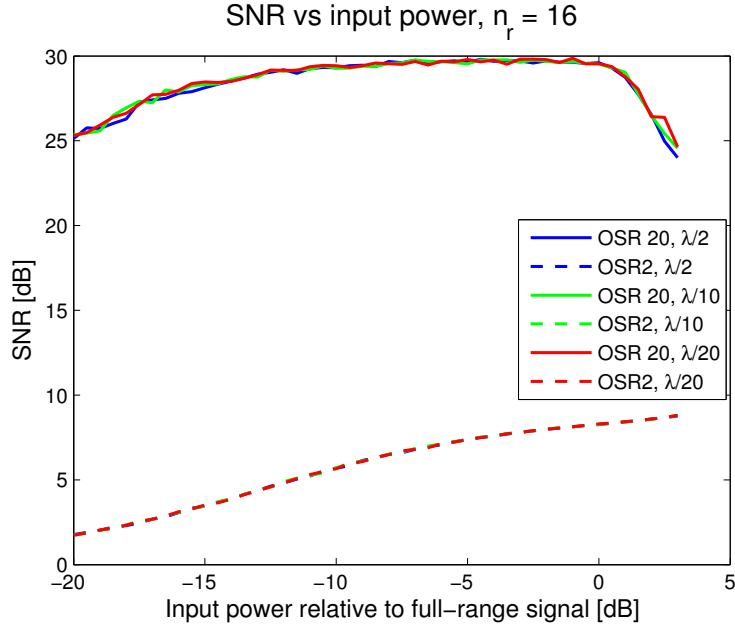


Figure 4.3: Reconstruction SNR vs. input power relative to full-range signal power for multiple ADCs in the context of beamforming for different antenna spacings and OSR. The input signal is bandlimited white noise, dither power is -37 dB relative to the signal power, number of antenna elements = 16, evaluation angle = 90 °. The results shown here are the mean values of 100 simulation runs for the spatio-temporal $\Sigma\Delta$ modulator.

4.3 Evaluation of reconstruction SNR vs. angle

The following simulations are made to show how a reconstructed signal's SNR value is related to beamforming direction for the three evaluated modulator structures. The beamforming is performed from 0 to 180 degrees with an angular resolution of 1 degree. Furthermore, the signal and noise portions are presented to show how these relate to the angle in order to explain why the SNR varies with the angle for some of the modulator structures. Lastly, for the cases where the SNR varies with the beamforming angle, plots are included to show that the noise can be shaped to certain angles in order to maximize the SNR for that beamforming angle.

The settings used in the simulations are presented in each of the captions. In general, the evaluations when applying white noise on each antenna are more realistic and should be paid more attention to than the noise free case. The noise free case is just included to provide further insight. Similarly, denser antenna spacings than the critical ($\lambda/2$) are included to show the impact of spatial oversampling.

The values of all beamforming sweeps in this section come from one simulation evaluation at each angle. Thus, the value at each angle is not a mean value of several simulation rounds but can instead be considered as a trend over the entire range from 0 to 180 degrees. This should be enough to detect if the SNR varies as a function of beamforming angle.

4.3.1 Temporal $\Sigma\Delta$ modulation

Figures 4.4 and 4.5 show that the SNR of the reconstructed signal does not depend on the angle of incidence. Figure 4.6 shows that the signal and noise portions are the same no matter the direction of the user. It is obvious that the SNR increases with dither added, which is expected as explained in the design chapter.

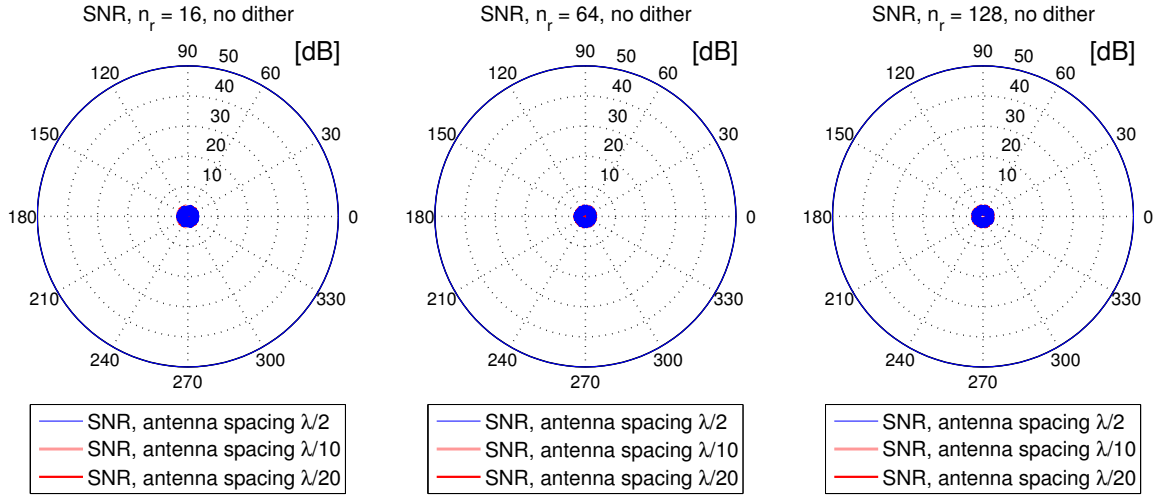


Figure 4.4: SNR for temporal $\Sigma\Delta$ modulation for a bandlimited white noise signal that represents a user signal when the antenna spacing distance is varied. Signal amplitude = 0.8, distance = 20, OSR = 2. No dither added. (a) number of antennas = 16 (b) number of antennas = 64 (c) number of antennas = 128.

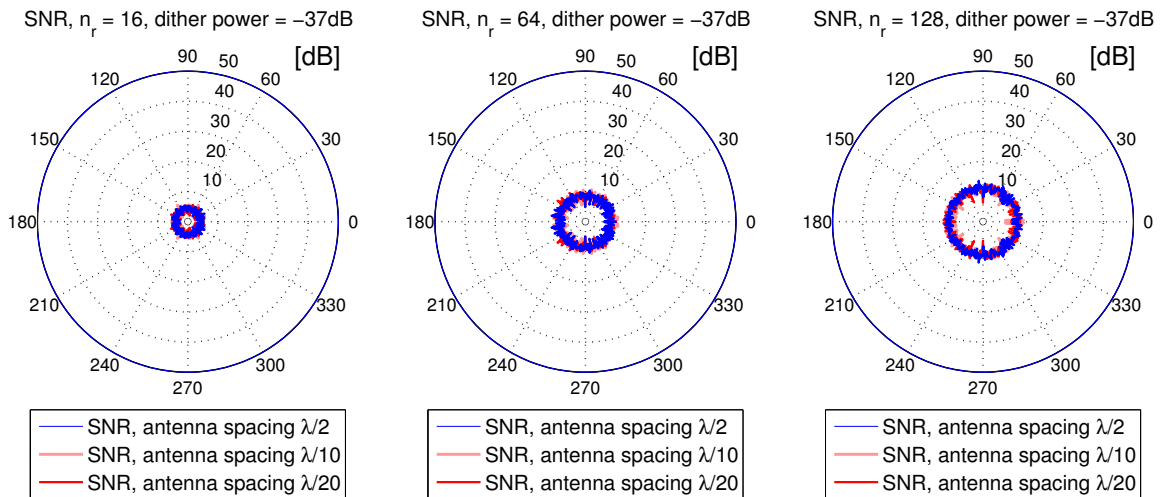


Figure 4.5: SNR for temporal $\Sigma\Delta$ modulation for a bandlimited white noise signal that represents a user signal when the antenna spacing distance is varied. Signal amplitude = 0.8, distance = 20, OSR = 2. Dither with power level = -37dB added. (a) number of antennas = 16 (b) number of antennas = 64 (c) number of antennas = 128.

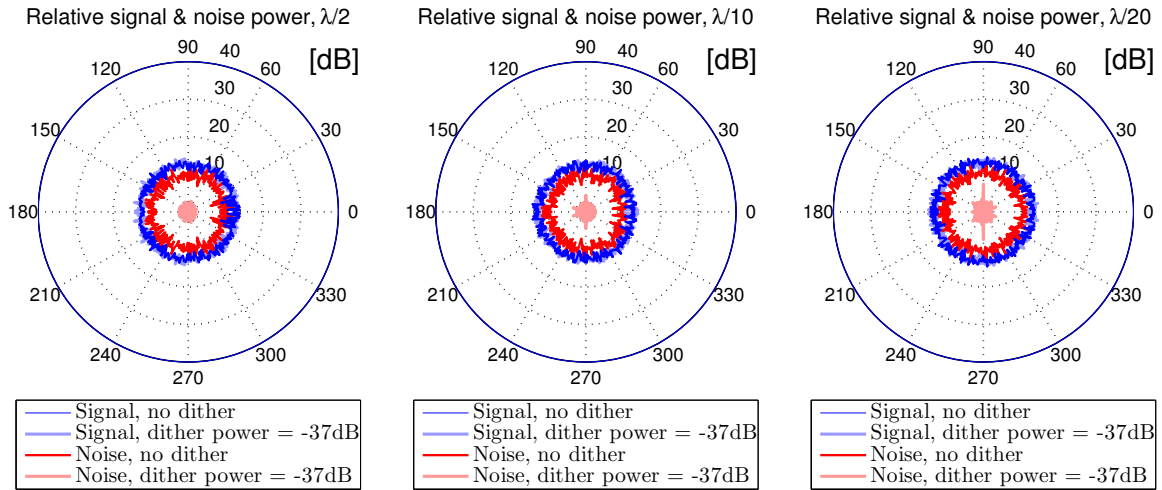


Figure 4.6: Comparison of relative signal and noise effect for temporal $\Sigma\Delta$ modulation, when a bandlimited white noise input signal is applied. Signal amplitude = 0.8, distance = 20, number of antennas = 128, OSR = 2. (a) antenna spacing = $\lambda/2$ (b) antenna spacing = $\lambda/10$ (c) antenna spacing = $\lambda/20$.

4.3.2 Spatial $\Sigma\Delta$ modulation

This sub section is divided in two parts; first, results of the first-order spatial $\Sigma\Delta$ modulator are presented and then results of a second-order implementation of the spatial $\Sigma\Delta$ modulator are shown.

Figures 4.7 and 4.8 show that the ability to reconstruct a transmitting user's data does depend on its angle relative to the antenna array center; this is spatial noise-shaping. Figure 4.9 shows that the signal and noise portions are different depending on beamforming direction. The noise is lowest in the direction 90 degrees which makes the SNR maximum for this angle.

Also note that the beamforming pattern shows a distinct SNR drop around the angle 120° when the antenna spacing is $\lambda/2$, in figures 4.7 and 4.8. There is also an SNR drop around 60° , but this is smoother. The SNR-drop effects around 60° and 120° diminish as the spatial oversampling increases (the antenna spacing is shorter), and the beamforming pattern gets a smoother curve form.

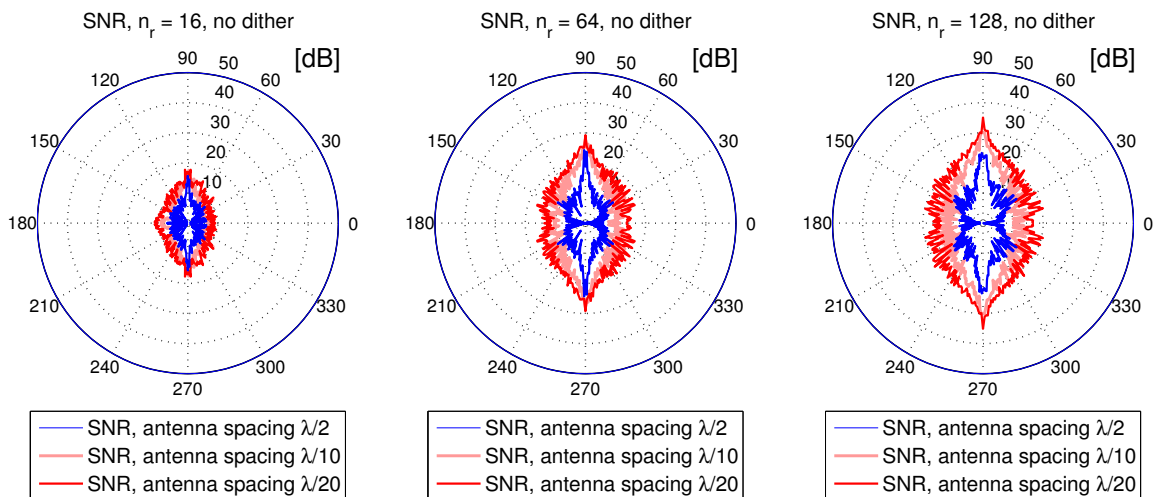


Figure 4.7: SNR for spatial $\Sigma\Delta$ modulation for a bandlimited white noise signal that represents a user signal when the antenna spacing distance is varied. Signal amplitude = 0.8, distance = 20, OSR = 2. No dither added. (a) number of antennas = 16 (b) number of antennas = 64 (c) number of antennas = 128.

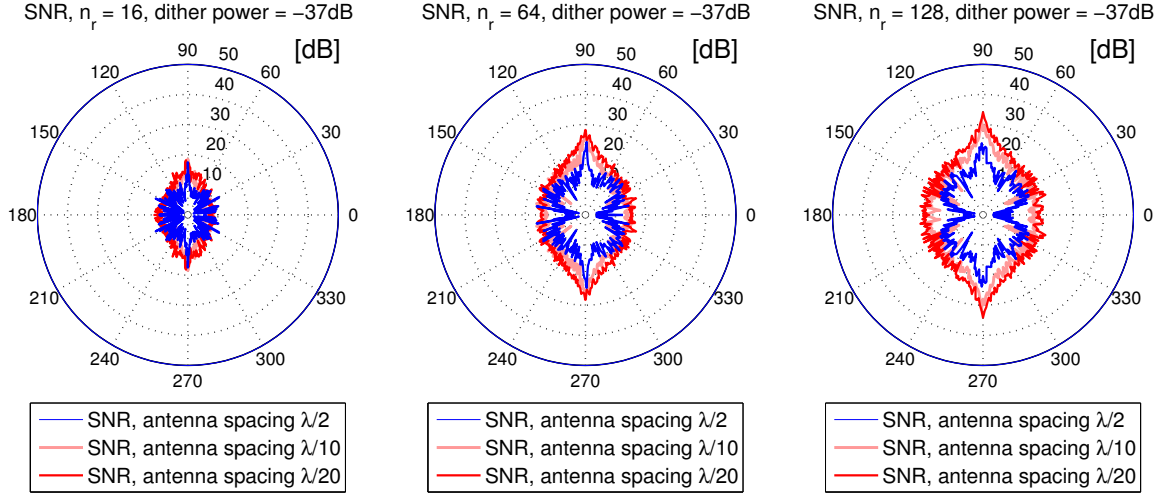


Figure 4.8: SNR for spatial $\Sigma\Delta$ modulation for a bandlimited white noise signal that represents a user signal when the antenna spacing distance is varied. Signal amplitude = 0.8, distance = 20, OSR = 2. Dither with power level = -37dB added. (a) number of antennas = 16 (b) number of antennas = 64 (c) number of antennas = 128.

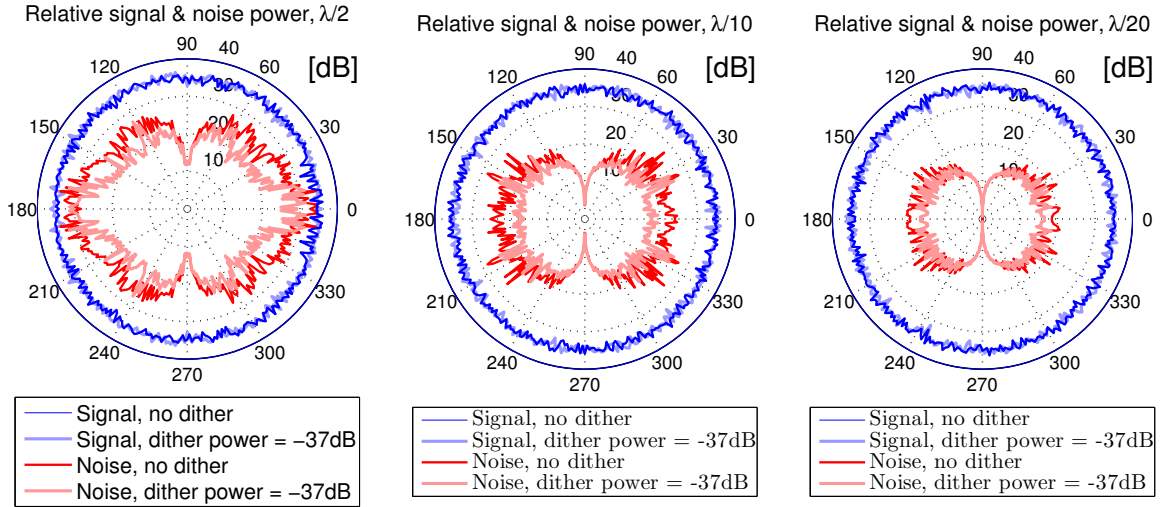


Figure 4.9: Comparison of relative signal and noise effect for spatial $\Sigma\Delta$ modulation, when a bandlimited white noise input signal is applied. Signal amplitude = 0.8, distance = 20, number of antennas = 128, OSR = 2. (a) antenna spacing = $\lambda/2$ (b) antenna spacing = $\lambda/10$ (c) antenna spacing = $\lambda/20$.

Figure 4.10 shows that it is possible to adjust the angle for which maximum SNR appears. This is done by shaping the noise to a minimum in that beamforming direction, using the proposed design in figure 2.22.

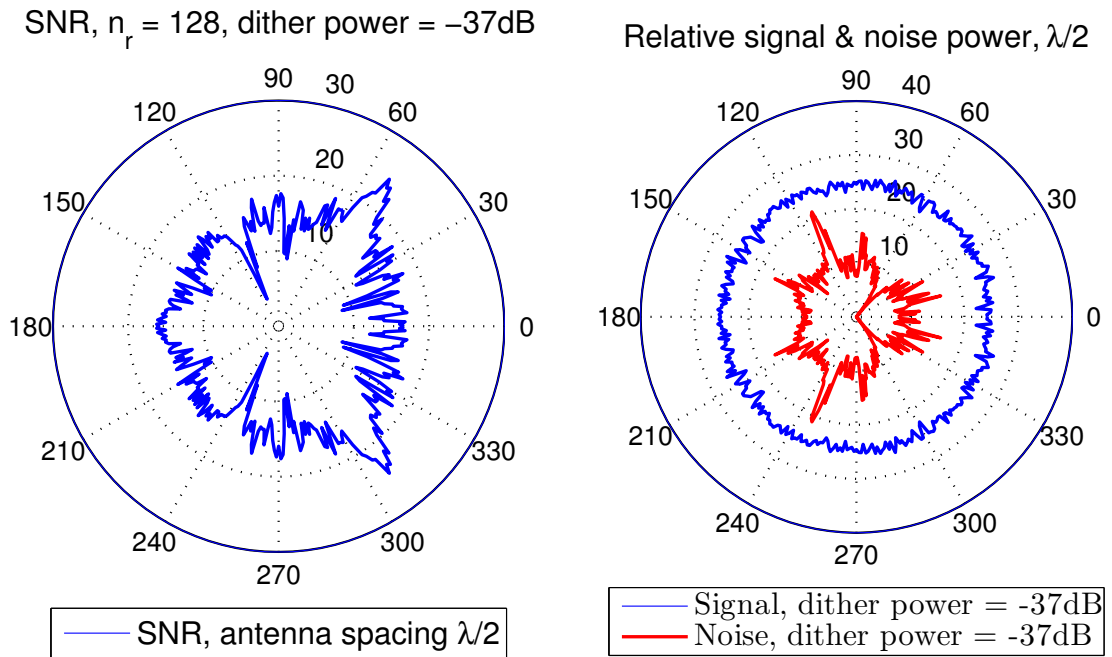


Figure 4.10: Spatial shaping of the noise for spatial $\Sigma\Delta$ modulation when a bandlimited white noise input signal is applied. The noise is intentionally minimized in the direction 50 degrees by delaying the quantization error. Signal amplitude = 0.8, distance = 20, number of antennas = 128, antenna spacing = $\lambda/2$, OSR = 2. Dither with power level = -37dB added. (a) SNR (b) Signal and noise portion

Spatial second-order $\Sigma\Delta$ modulator

Figure 4.11 shows the SNR reconstruction results when the second-order spatial $\Sigma\Delta$ modulator is used in the ADCs.

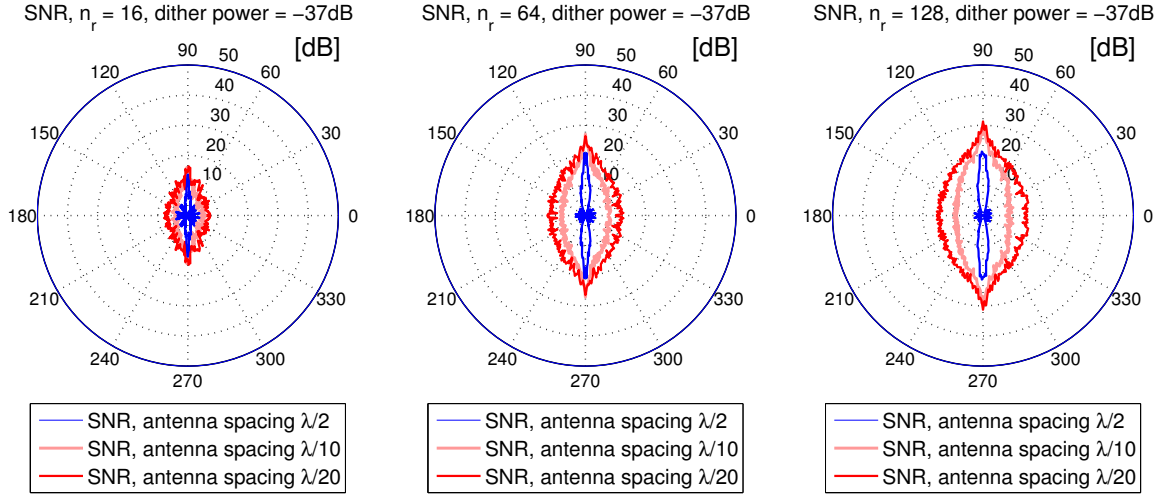


Figure 4.11: SNR for second-order spatial $\Sigma\Delta$ modulation for a bandlimited white noise signal that represents a user signal when the antenna spacing distance is varied. Signal amplitude = 0.8, distance = 20, OSR = 2. Dither with power level = -37 dB added, number of antennas = 128

Figures 4.12 a - c show a comparison between the first- and second-order $\Sigma\Delta$ modulators for three different antenna spacings. These figures are combinations of the different antenna spacings that can be seen in figure 4.8 c and figure 4.11 c respectively.

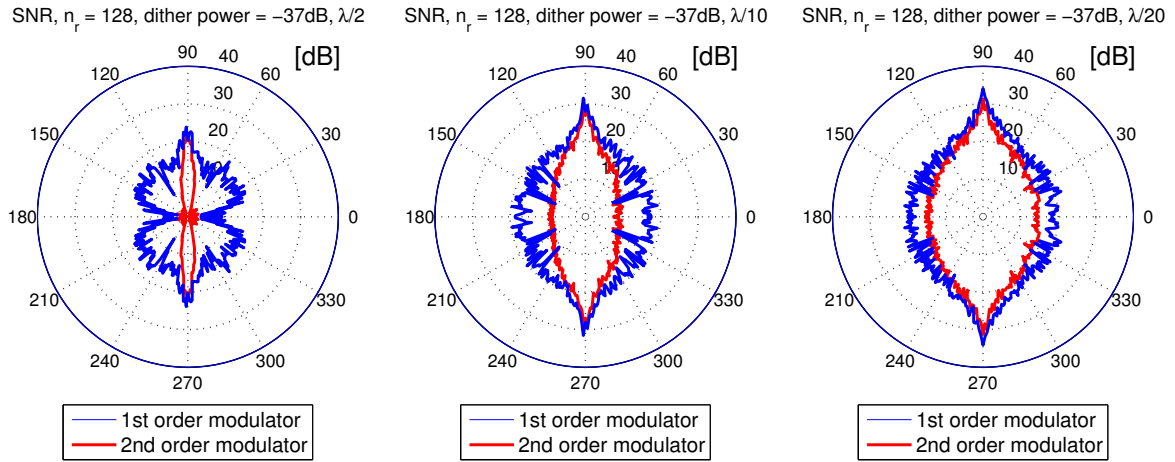


Figure 4.12: Comparison of the reconstruction SNR for the first- and second-order spatial $\Sigma\Delta$ modulator. The input signal is bandlimited white noise signal that represents a user signal when the antenna spacing distance is varied. Signal amplitude = 0.8, distance = 20, OSR = 2. Dither with power level = -37 dB added, number of antennas = 128

4.3.3 Spatio-temporal $\Sigma\Delta$ modulation

Figures 4.13 and 4.14 show that the ability to reconstruct a transmitting user's data does depend on its angle relative to the antenna array center. Figure 4.15 shows that the signal and noise portions are different depending on beamforming direction. The noise is lowest in the direction 90 degrees which makes the SNR maximum for this angle.

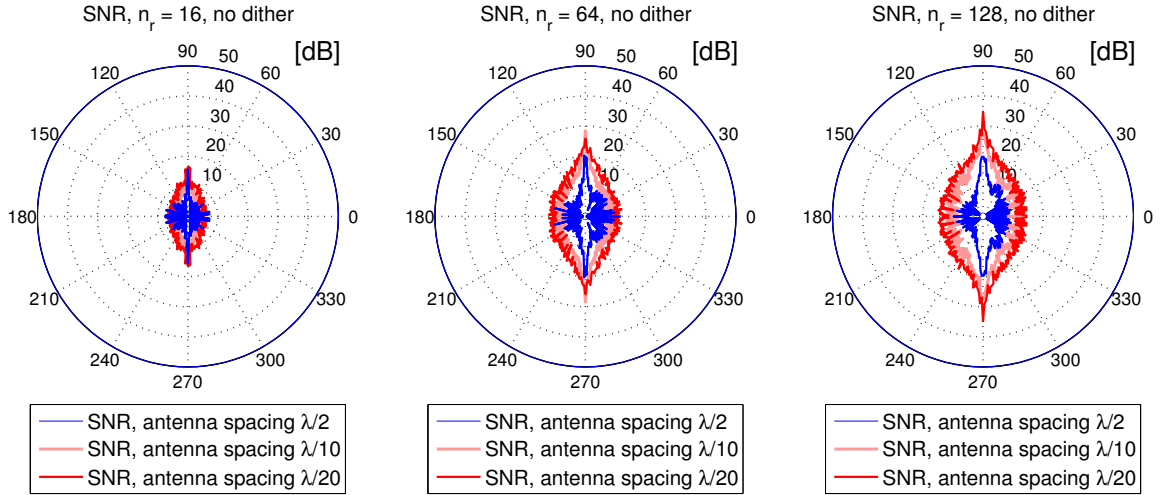


Figure 4.13: SNR for spatio-temporal $\Sigma\Delta$ modulation for a bandlimited white noise signal that represents a user signal when the antenna spacing distance is varied. Signal amplitude = 0.8, distance = 20, OSR = 2. No dither added. (a) number of antennas = 16 (b) number of antennas = 64 (c) number of antennas = 128.

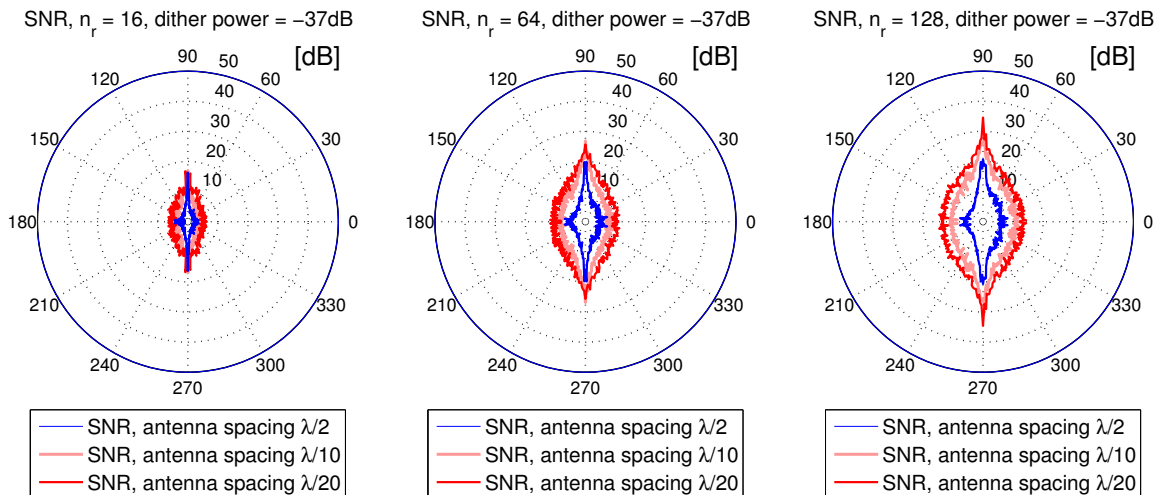


Figure 4.14: SNR for spatio-temporal $\Sigma\Delta$ modulation for a bandlimited white noise signal that represents a user signal when the antenna spacing distance is varied. Signal amplitude = 0.8, distance = 20, OSR = 2. Dither with power level = -37dB added. (a) number of antennas = 16 (b) number of antennas = 64 (c) number of antennas = 128.

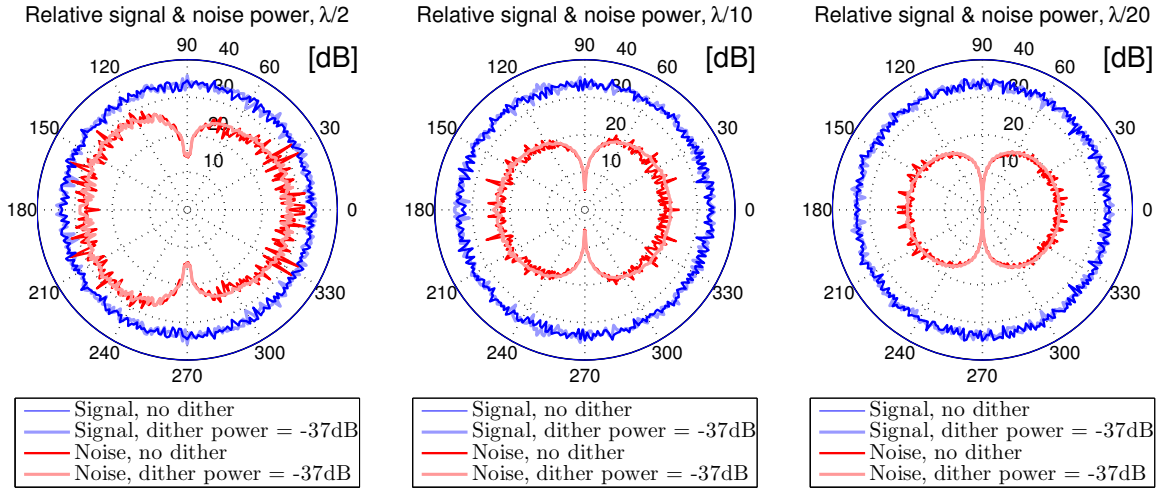


Figure 4.15: Comparison of relative signal and noise effect for spatio-temporal $\Sigma\Delta$ modulation, when a bandlimited white noise input signal is applied. Signal amplitude = 0.8, distance = 20, number of antennas = 128, OSR = 2. (a) antenna spacing = $\lambda/2$ (b) antenna spacing = $\lambda/10$ (c) antenna spacing = $\lambda/20$.

As in the spatial $\Sigma\Delta$ modulator it is possible to move the SNR peak. The design used was the one presented in figure 2.23, and figure 4.16 shows the simulation results.

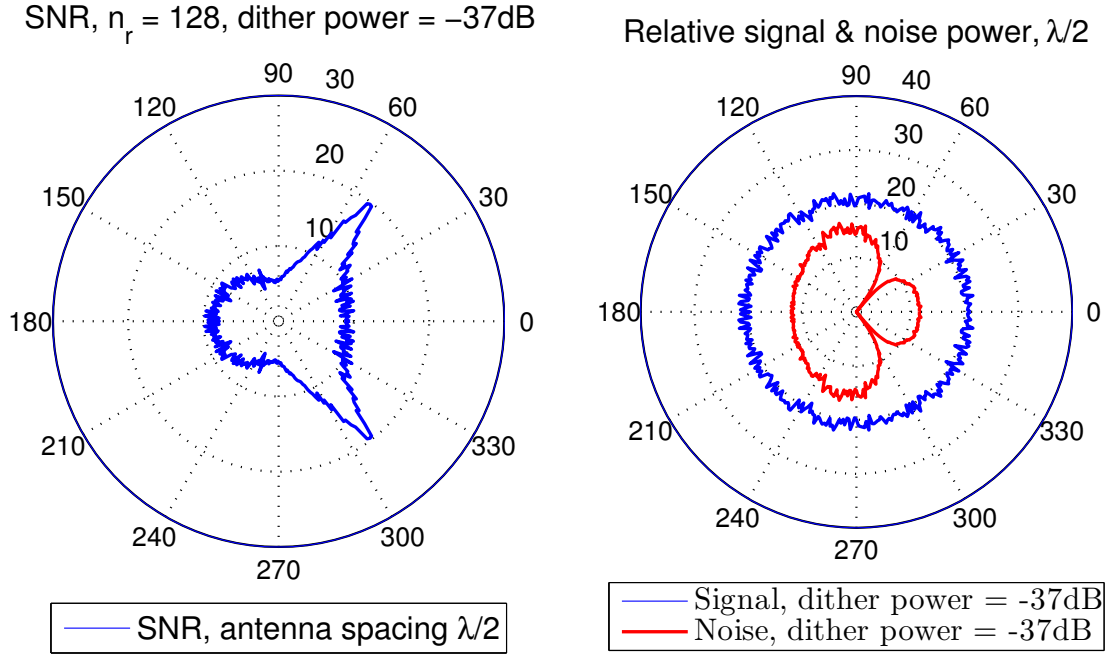


Figure 4.16: Spatial shaping of the noise for spatio-temporal $\Sigma\Delta$ modulation when a bandlimited white noise input signal is applied. The noise is intentionally minimized in the direction 50 degrees by delaying the quantization error. Signal amplitude = 0.8, distance = 20, number of antennas = 128, antenna spacing = $\lambda/2$, OSR = 2. Dither with power level = -37dB added. (a) SNR (b) Signal and noise portion

4.4 Comparison

The intention with this section is to analyze all modulator structures against each other rather than evaluating the properties of each structure. A multi-bit Nyquist quantizer is included as reference to answer the question regarding required data bandwidth. The evaluation spans from an OSR of 2 to an OSR of 8.

4.4.1 SNR comparison for low OSR

Figure 4.17 shows a combination of all three modulator structures that have been evaluated, and plotted together in one plot for easy comparison. The data from figures 4.5, 4.8 and 4.14 have been inserted together with a multi-bit Nyquist quantizer for comparison. For this low OSR of 2, the multi-bit Nyquist quantizer has the worst quality. Different antenna spacings have been evaluated as well to show the impact of denser spacing but the most important spacing is the critical one (antenna spacing = $\lambda/2$).

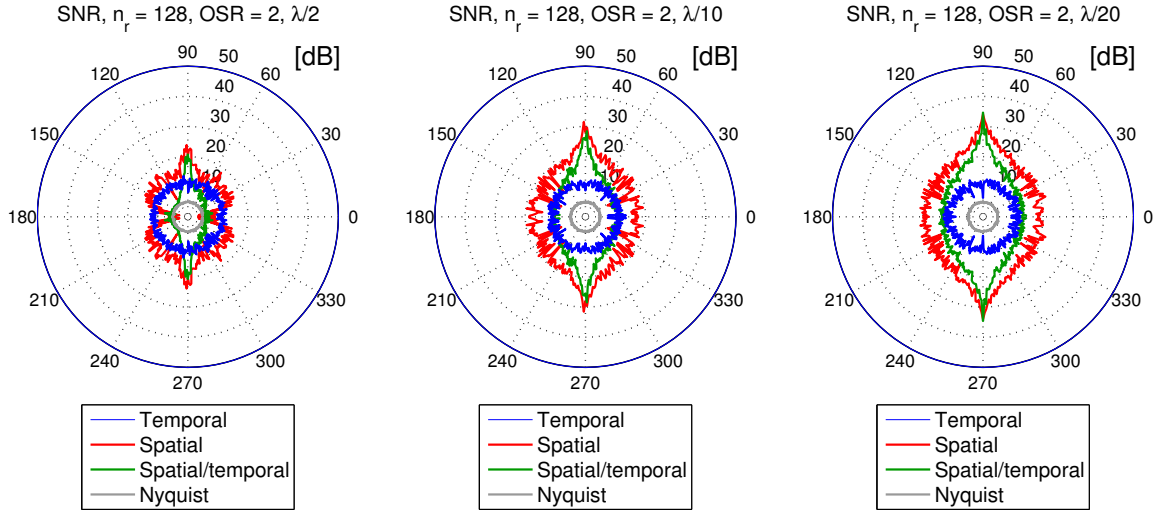


Figure 4.17: Comparison of the SNR for different modulator structures, when a bandlimited white noise input signal is applied. Signal amplitude = 0.8, distance = 20, number of antennas = 128, OSR = 2. Dither with power level = -37dB added. (a) antenna spacing = $\lambda/2$ (b) antenna spacing = $\lambda/10$ (c) antenna spacing = $\lambda/20$.

4.4.2 SNR comparison for high OSR

Figure 4.18 shows a comparison of all three modulator structures together with a reference multi-bit Nyquist quantizer. For this high OSR of 8, the multi-bit Nyquist quantizer has the best quality.

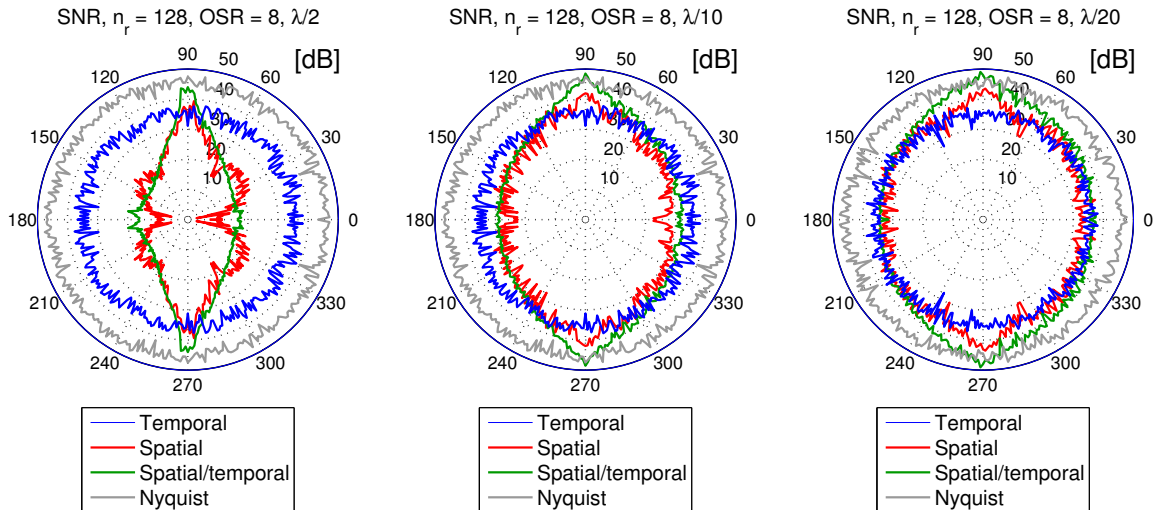


Figure 4.18: Comparison of the SNR for different modulator structures, when a bandlimited white noise input signal is applied. Signal amplitude = 0.8, distance = 20, number of antennas = 128, OSR = 8. Dither with power level = -37dB added. (a) antenna spacing = $\lambda/2$ (b) antenna spacing = $\lambda/10$ (c) antenna spacing = $\lambda/20$.

4.4.3 SNR trend

Figure 4.19 shows the peak SNR for the evaluated modulator structures as well as the reference multi-bit Nyquist quantizer, for different values of temporal OSR. The evaluation was set up with an antenna spacing distance of $\lambda/2$, 128 antennas and a distance of 20 m between the user source and the antenna array center. Dither with power level = -37dB was added to represent antenna noise. Each dot for each modulator in the trend corresponds to the mean value of 100 simulation evaluations at the angle 90 degrees (straight in front of the antenna array center) in order to determine the peak SNR.

The choice of using the critical antenna spacing distance $\lambda/2$ is related to the precision or ability to distinguish multiple users. From the previously presented evaluations it is clear that some modulator structures' SNR improve when the antenna spacing is denser and it might seem tempting to evaluate the modulators when having these denser spacings to achieve better SNR. If the antenna spacing would have been denser than $\lambda/2$, this would have the effect that the antenna array length would be smaller and the ability to distinguish multiple users would be reduced. This is the reason why the modulators have been evaluated at $\lambda/2$.

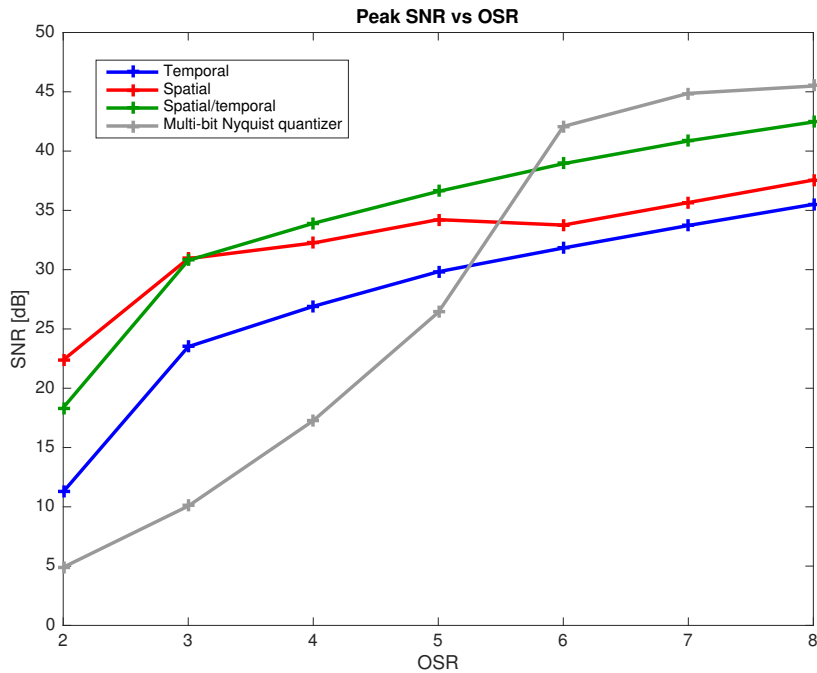


Figure 4.19: SNR vs. bandwidth comparison for the different evaluated ADC designs.

4.4.4 Bandwidth

The data shown in figure 4.20 is in fact the same as the data in figure 4.19. The only difference is that the x- and y-axis have been swapped. The value on the y-axis tells how many bits are required to produce a certain SNR for any of the four modulator structures. For instance, the required number of bits per sampling time to produce the

SNR of about 18 dB is 2 for the spatio-temporal $\Sigma\Delta$ modulator while the number of bits for the multi-bit Nyquist quantizer is 4. This means that the spatio-temporal $\Sigma\Delta$ modulator is 2 times more efficient in terms of bandwidth. The spatial $\Sigma\Delta$ modulator produces an SNR of around 23 dB for 2 bits per sampling time and in order to achieve at least this SNR, the multi-bit Nyquist quantizer needs at least 4.5 bits of resolution which makes the spatial $\Sigma\Delta$ modulator 2.25 times as efficient as the multi-bit Nyquist quantizer. The bandwidth is thus reduced to 0.5 and 0.44 respectively of the bandwidth that a multi-bit Nyquist quantizer requires. Similarly, the temporal $\Sigma\Delta$ modulator requires about 2.5 bits to achieve an SNR of around 20 dB which corresponds to 0.63 of the bandwidth that a multi-bit Nyquist quantizer needs.

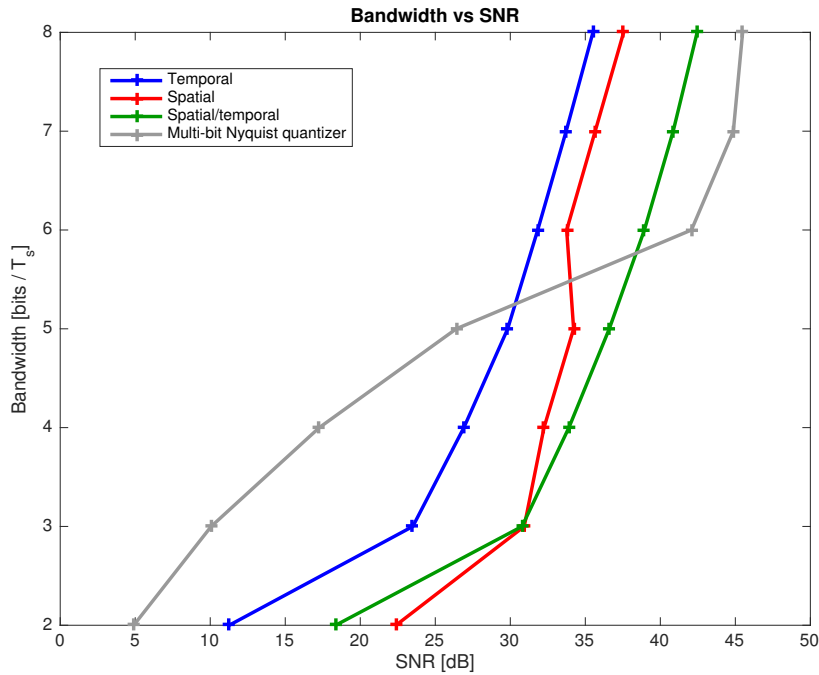


Figure 4.20: SNR vs. bandwidth comparison for the different evaluated ADC designs.

4.5 Multi-user analysis

The reason to perform the following tests is to evaluate the applicability of each of the investigated modulator structures in a setup of multiple users. More specifically, it is necessary to show that the different users in a multi-user setup can be sufficiently distinguished from each other, and that the observed signal qualities in the single-user case is also valid in the presence of multiple users. Merely showing that the SNR in one direction is better for one modulator structure than another does not automatically mean that it actually works better.

There are two cases for each user signal; an ideal case and a multi-user case. The ideal case means that one user is placed at a certain position which is determined by the distance and angle of incidence to the antenna array center. No other user sources are present. This scenario is then run 100 times for each of the 5 users in isolation and the mean

value of the SNR in the range 0 to 180 degrees is then calculated. These ideal plots are combined in the same plot with the same color (red). The multi-user case is similar, but with the difference that all 5 users are placed simultaneously in the configuration. This means that the evaluated SNR in this case shows if any of the adjacent users' signal transmission affect the signal reconstruction for a certain user.

This evaluation is performed as having 5 users placed at a distance of 20 m from the antenna array center and with certain angles of incidence. The angles are 50, 50.5, 90, 100 and 105 degrees respectively for all three cases below. In all tests, the antenna spacing distance is $\lambda/2$.

The signal amplitudes of the users in these tests have been scaled down with a factor 5 so that the total superpositioned signal amplitude is not larger than 0.8. This is equivalent with reducing the gain of the antenna elements to avoid clipping. All users transmit with the same signal strength. In addition, the dither power level was reduced to -30dB relative to the input signal power.

The red curves indicate the ideal SNR for a certain user at a certain angle when no other source is present. The blue curves indicate the real or actual SNR value in that user direction when all 5 user sources are present. Comparing the red and blue curves show how the adjacent users' signals interfere with a certain user's SNR; if the red and blue curve match then there is no or small interference. The gray curve indicates the RMS value. The RMS value is intended to show that the antenna array is subjected to a wide signal contribution from all users. The red and blue curves are expressed in dB while the RMS is unitless and indicates the entire signal content in the range 0 to 180 degrees.

The plots are presented in two ways; one plot shows the full content from all signals, both the ideal and the multi-user case. Furthermore, the RMS is shown in the same plot. An example of this is figure 4.21 a. The other plot shows each of the signals but only a partial portion for the angle where the user is placed. For instance, the data caused by the user at 50 degrees is provided for the angles 48 to 52 degrees, the remaining angles' SNR value are all set to 0. The intention with this is to make the plots clearer since there is always some SNR detection in the adjacent directions. An example of this is shown in figure 4.21 b.

4.5.1 Temporal $\Sigma\Delta$ modulation

Figure 4.21 a shows the entire content for the 5 users. Although the antenna detects a large amount of signal power (RMS), the users can be distinguished with little SNR reduction which is clear from figure 4.21 b.

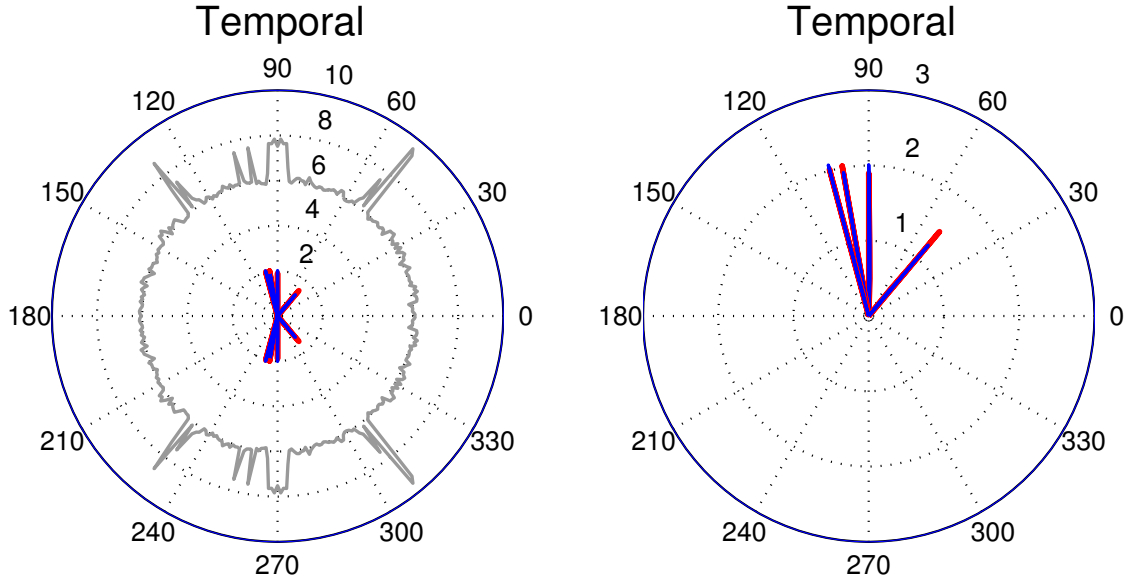


Figure 4.21: A multi-user case scenario with 5 users placed in a certain arrangement when the temporal $\Sigma\Delta$ modulator is used. Signal amplitudes = $0.8/5$, distance = 20, number of antennas = 128, antenna spacing = $\lambda/2$, OSR = 2. Dither with power level = -30dB relative to the input signal power. (a) Entire content (b) Partial content

4.5.2 Spatial $\Sigma\Delta$ modulation

Figure 4.22 suggests that spatial $\Sigma\Delta$ modulation deviates significantly from the ideal behavior. Note that there is very much content from the red lines. This indicates that the spatial structure is not consistent in a multi-user setup. It might work better if the antenna spacing is denser than the critical distance $\lambda/2$ which corresponds to spatial oversampling. This is supported from figures 4.7 and 4.8, which indicate beamforming reconstruction problems around 120° for the antenna spacing of $\lambda/2$.

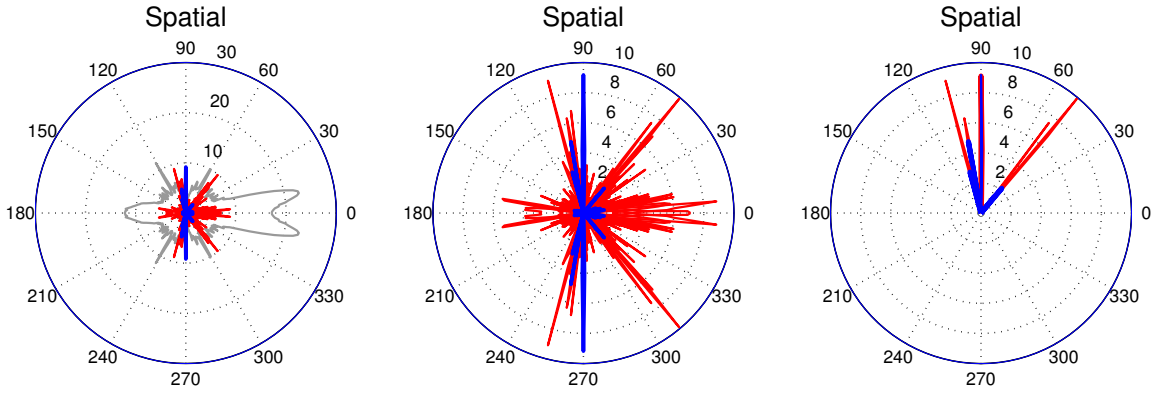


Figure 4.22: A multi-user case scenario with 5 users placed in a certain arrangement when spatial $\Sigma\Delta$ modulation is used. Signal amplitudes = $0.8/5$, distance = 20, number of antennas = 128, antenna spacing = $\lambda/2$, OSR = 2. Dither with power level = -30dB relative to the input signal power. (a) Entire content (b) Entire content zoomed (c) Partial content

4.5.3 Spatio-temporal $\Sigma\Delta$ modulation

Figure 4.23 indicates that spatio-temporal $\Sigma\Delta$ modulation works well in a multi-user environment.

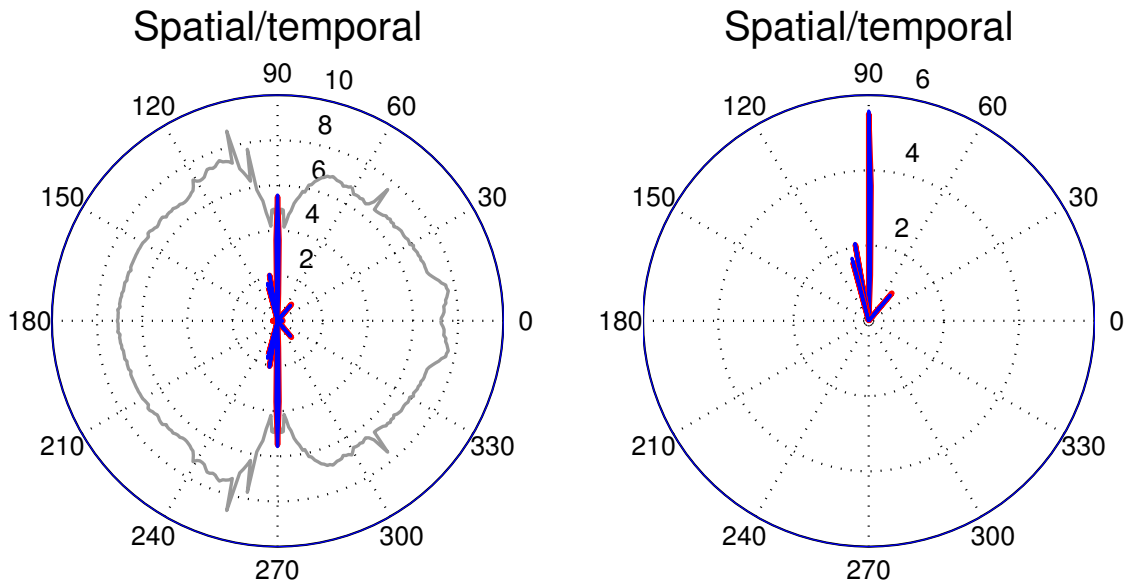


Figure 4.23: A multi-user case scenario with 5 users placed in a certain arrangement when spatio-temporal $\Sigma\Delta$ modulation is used. Signal amplitudes = $0.8/5$, distance = 20, number of antennas = 128, antenna spacing = $\lambda/2$, OSR = 2. Dither with power level = -30dB relative to the input signal power. (a) Entire content (b) Partial content

Chapter 5

Discussion

5.1 Observations and findings

An insight from the simulation results is that the use of spatial and spatio-temporal $\Sigma\Delta$ modulation have the ability to improve the signal reconstruction SNR straight in front of the antenna array, and even better with increasing number of antennas. Smaller antenna spacing also improves the reconstruction SNR, which is probably due to the fact that it represents spatial oversampling. However the effect is only visible with a large amount of antenna elements; for 64 and 128 antennas in our simulations. In addition, denser antenna spacing improves the SNR at angles far from 90 degrees. It is also shown in the investigation that the angle for which maximum SNR is achieved, can be shaped to other angles than straight in front of the antenna array. This is accomplished by inserting delays between the ADC rows to compensate for the delay difference imposed by the beamforming. The temporal $\Sigma\Delta$ modulator ADC and the multi-bit Nyquist quantizer doesn't improve with denser antenna spacing, although they improve with increasing number of antennas.

Another interesting finding is that a moderate amount of dither, or applied antenna noise, improves the beamforming reconstruction SNR for the temporal modulator structure while it slightly degrades the performance for the spatial modulator structure. These observations were made when searching for an appropriate amount of dither. In a real implementation, white noise is unavoidable. This means that one design improves by naturally generated white noise, while another degrades. Obviously if there's a large amount of dither, all designs perform worse.

It was discovered that for an OSR of two, the reconstruction SNR is not degraded for input amplitudes that exceed 1.0. In fact, the SNR of the temporal and spatio-temporal $\Sigma\Delta$ modulators increases with the amplitude, at least for signal powers up to 3 dB above the full-range signal. The SNR of the spatial $\Sigma\Delta$ modulator does not increase beyond amplitude levels of 1.0 but the SNR does not degrade either; it is more or less constant. This indicates that analog-to-digital conversion in the context of beamforming is beneficial for low OSR values. For a higher OSR value of 20, the SNR decreased beyond an input amplitude of 1.0 which is in accordance with the behavior of a single $\Sigma\Delta$ modulator. The

antenna spacing distance does not have any influence on the resulting SNR vs. input power for either OSR.

A second-order spatial $\Sigma\Delta$ modulator was successfully implemented and evaluated for comparison with a first-order spatial $\Sigma\Delta$ modulator. There were no obvious benefits compared to the first-order design. The main difference is that the 2nd order modulator has a more narrow beamforming pattern than the 1st order modulator, but that they are otherwise very similar. The anticipated widening of the angle range in which the SNR is good could not be seen.

5.2 Limitations

The biggest drawback with using the spatial dimension in a $\Sigma\Delta$ modulator is the fact that the reconstruction SNR is mostly improved straight in front of the antenna array center and that it drops fast in other angles. While it is indeed possible to move this direction, it might require quite complex analog phase shifters between the ADCs which would defeat the entire purpose of using the $\Sigma\Delta$ modulator for its simple components. In addition, it's currently only one direction. One issue with the compensation delay in the error forwarding connection is that the delay will need to be non causal if the user is at an angle larger than 90° , if the error is propagated top to bottom where top represents user position 0° . Possible solutions to this could be to somehow enable the possibility to reverse the direction of the spatial delay and select the configuration that is causal, consider antenna shapes that might solve the problem or to redesign the error forwarding connection to make it more flexible.

Looking beyond the limitation of directions, another possible limitation with using the spatial dimension in a $\Sigma\Delta$ modulator is the limited signal propagation speed. It might be desirable to place respective ADC very close to the antenna to reduce antenna cable crosstalk, signal quality loss, reflections and such. In that case, if a spatial $\Sigma\Delta$ modulator is used, the error has to propagate from the top to the bottom of the array before the next quantization can take place, limiting the sampling frequency. In a case with antenna spacing $\frac{\lambda}{2}$, carrier frequency 800 MHz, 128 antennas, a one-dimensional antenna and a speed of electricity of $0.64c$ [22], the propagation delay of the error counting only the wires restricts the sampling frequency to 8 MHz. This makes sampling a base signal with bandwidth 20 MHz not possible at all. Adding to that charging and discharging of capacitances and other things on the way that delays the signal, it looks even darker. Considering a carrier frequency of 5 GHz, we get a clock restriction of 50 MHz by the wire propagation delay, indeed possibly allowing for an OSR of two, but leaving very little room for other delays on the way. One possible way to move beyond this is to arrange the spatial $\Sigma\Delta$ modulator into groups, having many partial parallel ADCs.

5.3 Future work

Coming back to the original purpose, which is reducing the bandwidth, it is clear that there are benefits with using the spatial dimension in a $\Sigma\Delta$ modulator. It is however obvious that the investigation calls for future work. The quite serious drawbacks of the spatial and spatio-temporal $\Sigma\Delta$ modulator needs to be addressed to be usable in a real case. One question we asked ourselves is if it's possible to listen in two directions simultaneously with only one set of delay between the antenna elements. If this is possible, it might also be possible to shape the error in multiple directions simultaneously with only one delay in the error forwarding connection. There has been one successful trial in a transmit array to form multiple beams with only varying the phase of each antenna element. The delays were obtained through using particle swarm optimization [23]. However, inserting delay in the error forwarding connection requires a delay implemented in analog circuitry which may or may not be feasible or desirable.

There are many tracks which could be taken throughout the course of this master thesis project. This investigation is undoubtedly a comparatively simple use of the spatial dimension; it seems very reasonable that it's possible to take advantage of the antenna array system in multiple other ways which may be better. For instance, the signals at one antenna is going to be very correlated to the adjacent antennas; in our work the spatial correlation hasn't been exploited at all. It might be possible to do something similar to image compression, or to use the difference between two signals which possibly will be smaller than one signal on its own. To conclude, there is an abundance of interesting research topics on the subject of antenna arrays.

Chapter 6

Conclusion

Three $\Sigma\Delta$ modulator designs have been investigated: the temporal, the spatial, and the spatio-temporal which is a combination of the first two. At low OSR the spatial $\Sigma\Delta$ modulator is the best performing of the bunch, with an improvement of 17 dB compared to the conventional multibit Nyquist quantizer. At higher OSR the spatio-temporal $\Sigma\Delta$ modulator outperforms all the other $\Sigma\Delta$ modulator designs, with a constant improvement of about 6 dB compared to the temporal $\Sigma\Delta$ modulator. At OSR lower than six all the $\Sigma\Delta$ modulators outperform the corresponding multi-bit Nyquist quantizer, while above it's the other way around.

The original purpose was to reduce the bandwidth needed for a certain SNR requirement. Assuming a multi-bit Nyquist quantizer as a reference ADC and an SNR requirement of 20 dB, using the spatial $\Sigma\Delta$ modulator lowers the bandwidth requirement to about 0.44 times the bandwidth required of the multi-bit Nyquist quantizer; the spatio-temporal $\Sigma\Delta$ modulator requires 0.5 of the bandwidth. The temporal $\Sigma\Delta$ modulator does not have the same ability to provide high reconstruction SNR but it can still reduce the bandwidth to about 0.63 of the bandwidth required from a multi-bit Nyquist quantizer. Besides this, the temporal modulator structure does not have the limitation that it only works well in a certain direction.

There are certain limitations with the designs studied. From the real case investigation of the spatial $\Sigma\Delta$ modulator it is clear that in the presence of multiple users the performance is dramatically worse for users positioned to the side, as compared to if the user was alone in the system. This issue is not seen in the temporal and spatial $\Sigma\Delta$ modulator design. Another limitation with using the spatial dimension in the $\Sigma\Delta$ modulator is that the SNR is good only in one quite narrow direction, and although it is possible to move it, it's currently still only one direction.

Bibliography

- [1] D. Tse and P. Viswanath, *Fundamentals Of Wireless Communication*. Cambridge, N.Y: Cambridge UP, 2005.
- [2] Ericsson. Ericsson 5G Radio Prototypes for live field trials. [Online]. Available: <https://youtu.be/5naPdaSRVNA>
- [3] P. Upadhyaya, J. Savoj, F. T. An, A. Bekele, A. Jose, B. Xu, D. Wu, D. Furker, H. Aslanzadeh, H. Hedayati, J. Im, S. W. Lim, S. Chen, T. Pham, Y. Frans, and K. Chang, “3.3 a 0.5-to-32.75gb/s flexible-reach wireline transceiver in 20nm cmos,” in *2015 IEEE International Solid-State Circuits Conference - (ISSCC) Digest of Technical Papers*, Feb 2015, pp. 1–3.
- [4] E. Larsson, O. Edfors, F. Tufvesson, and T. Marzetta, “Massive MIMO for next generation wireless systems,” *Communications Magazine, IEEE*, vol. 52, no. 2, pp. 186–195, February 2014.
- [5] Y. Joo, J. Park, M. Thomas, K. S. Chung, M. A. Brooke, N. M. Jokerst, and D. S. Wills, “Smart CMOS focal plane arrays: a Si CMOS detector array and sigma-delta analog-to-digital converter imaging system,” *IEEE Journal of Selected Topics in Quantum Electronics*, vol. 5, no. 2, pp. 296–305, Mar 1999.
- [6] I. Galton and H. T. Jensen, “Delta-Sigma modulator based A/D conversion without oversampling,” *IEEE Transactions on Circuits and Systems II: Analog and Digital Signal Processing*, vol. 42, no. 12, pp. 773–784, Dec 1995.
- [7] D. Palguna, D. J. Love, T. Thomas, and A. Ghosh, “Millimeter Wave Receiver Design Using Parallel Delta Sigma ADCS and Low Precision Quantization,” in *2015 IEEE Globecom Workshops (GC Wkshps)*, Dec 2015, pp. 1–7.
- [8] S. Norsworthy, R. Schreier, G. Temes, and I. C. . S. Society, *Delta-Sigma data converters: theory, design, and simulation*. IEEE Press, 1997.
- [9] S. Noujaim, S. Garverick, and M. O’Donnell, “Phased array ultrasonic beam forming using oversampled A/D converters,” Apr. 20 1993, US Patent 5,203,335. [Online]. Available: <http://www.google.se/patents/US5203335>
- [10] H. Aomori, T. Otake, N. Takahashi, and M. Tanaka, “Sigma-delta cellular neural network for 2D modulation,” *Neural Networks*, 2008.

- [11] M. Kozak and M. Karaman, “Digital phased array beamforming using single-bit delta-sigma conversion with non-uniform oversampling,” *Ultrasonics, Ferroelectrics, and Frequency Control, IEEE Transactions on*, vol. 48, no. 4, pp. 922–931, July 2001.
- [12] Y. Tamura, N. Kawakami, O. Akasaka, M. Okada, and K. Koyama, “Beam-forming using multidimensional sigma-delta modulation,” in *Ultrasonics Symposium, 1998. Proceedings., 1998 IEEE*, vol. 2, 1998, pp. 1077–1080 vol.2.
- [13] B. V. Veen and K. M. Buckley, “Beamforming: a versatile approach to spatial filtering,” *IEEE ASSP Magazine April 1988*, 1988.
- [14] D. B. Smith and T. D. Abhayapala, “Maximal Ratio Combining Performance Analysis in Spatially Correlated Rayleigh Fading Channels with Imperfect Channel Knowledge,” in *2005 Asia-Pacific Conference on Communications*, Oct 2005, pp. 549–553.
- [15] F. Maloberti, *Data Converters*. Springer, 2007.
- [16] T. Xu and M. Condon, “Comparative study of the MASH digital delta-sigma modulators,” in *Research in Microelectronics and Electronics, 2009. PRIME 2009. Ph.D.*, July 2009, pp. 196–199.
- [17] Y. Tamura, O. Akasaka, and M. Okada, “Wavefront Generation Using a Dense Array and Multidimensional Delta-Sigma modulation,” *Japanese Journal of Applied Physics*, vol. 36, no. 5S, p. 3053, 1997.
- [18] G. mobile Suppliers Association, “Evolution of LTE Report: 4G Market & Technology Update,” Global mobile Suppliers Association, Report, October 2015. [Online]. Available: http://gsacom.com/wp-content/uploads/2015/10/151013-Evolution_to_LTE_report.pdf
- [19] LTE. [Online]. Available: <http://www.3gpp.org/technologies/keywords-acronyms/98-lte>
- [20] P. M. Sainju, “LTE Performance Analysis on 800 and 1800 MHz Bands,” Master’s thesis, Tampere University of Technology, 2012.
- [21] (2008, May). [Online]. Available: <http://www.enterprisenetworkingplanet.com/netsp/article.php/3747656/WiFi-Define-Minimum-SNR-Values-for-Signal-Coverage.htm>
- [22] Y. Li, *Computer Principles and Design in Verilog HDL*. Tsinghua University Press, 2015.
- [23] P. Nayeri, F. Yang, and A. Z. Elsherbeni, “Design of Single-Feed Reflectarray Antennas With Asymmetric Multiple Beams Using the Particle Swarm Optimization Method,” *IEEE Transactions on Antennas and Propagation*, vol. 61, no. 9, pp. 4598–4605, Sept 2013.